J. Chem. Thermodynamics 136 (2019) 59–76

Contents lists available at ScienceDirect

J. Chem. Thermodynamics

journal homepage: www.elsevier.com/locate/jct

Phase stability conditions for clathrate hydrate formation in (fluorinated refrigerant + water + single and mixed electrolytes + cyclopentane) systems: Experimental measurements and thermodynamic modelling

Peterson Thokozani Ngema [a,b], Paramespri Naidoo [a], Amir H. Mohammadi [a,*], Deresh Ramjugernath [a,*]

[a] Thermodynamics Research Unit, School of Engineering, University of KwaZulu-Natal, Howard College Campus, King George V Avenue, Durban 4041, South Africa
[b] Durban University of Technology, Department of Chemical Engineering, Thermodynamics Research Group, Steve Biko Campus, Durban 4001, South Africa

ARTICLE INFO

Article history:
Received 29 September 2018
Received in revised form 15 April 2019
Accepted 16 April 2019
Available online 17 April 2019

Keywords:
Gas hydrate
Clathrate hydrate
Water desalination
Refrigerant
Salt
Phase equilibrium

ABSTRACT

Phase equilibrium conditions (dissociation data) for clathrate hydrates (gas hydrates) were studied for systems involving fluorinated refrigerants + water + single and mixed electrolytes (NaCl, $CaCl_2$, $MgCl_2$ and Na_2SO_4) at varying salt concentrations in the absence and presence of cyclopentane (CP). The ternary systems for (R410a or R507) + water + CP were performed in the temperature and pressures ranges of (279.8–294.4) K and (0.158–1.385) MPa, respectively. Measurements for {R410a + water + (NaCl or $CaCl_2$) + CP} were undertaken at salt concentrations of (0.10, 0.15 and 0.20) mass fractions in the temperature and pressure ranges of (278.4–293.7) K and (0.214–1.179) MPa, respectively. The temperature and pressure conditions for the (R410a + water + Na_2SO_4) system were investigated at salt concentration of 0.10 mass fraction in range of (283.3–291.6) K and (0.483–1.373) MPa respectively. Measurements for {(R410a or R507) + water + mixed electrolytes NaCl, $CaCl_2$, $MgCl_2$} were undertaken at various salt concentrations of (0.002–0.15) mass fractions in the temperature and pressure ranges of (274.5–292.9) K and (0.149–1.119) MPa in the absence and presence of CP, for which there are no published data related to mixed salt and a promoter. The phase equilibrium measurements were performed using a non-visual isochoric equilibrium cell and the pressure-search technique. This study was focused on obtaining equilibrium data that can be utilized to design and optimize for water desalination process and the development of a Hydrate Electrolyte–Cubic Plus Association (HE–CPA) Equation of State based model. The results indicate hydrate dissociation pressure reduction/hydrate dissociation temperature increase up to ambient conditions in the presence of promoter (CP). The experimental results were then modelled. The modelling results are in good agreement with the measured hydrate dissociation data.

1. Introduction

Gas hydrates, or clathrate hydrates, have gained potential to produce pure/clean water that can be used for drinking as well as for industrial or agricultural purposes, due to their advantages of utilizing lower energy consumption in comparison with the reverse osmosis (RO) and multistage flash distillation (MSF) [1–4]. Gas hydrate technology shows a potential as a future technique to be employed at industries to purify wastewater and seawater. Gas hydrates are like a crystal solid structure which consists of water molecules which form cage structures due to hydrogen bonding at elevated high pressures and temperatures [1–7]. Generally, two types of crystalline gas hydrate structures were initially detected which were classified as structure I (sI) and structure II (sII). Later, a third structure, H (sH), was detected by Ripmeester *et al.* [8], but it is less common. The details pertaining to the characteristics of these structures can be found elsewhere [3].

Sea water and industrial wastewater contain certain concentration of common salts which typically include NaCl, $MgCl_2$, $CaCl_2$ and Na_2SO_4 that are required to be eliminated from the water [4,9–22]. The traditional desalination processes such as RO and MSF are used to eliminate salt from water, while these processes are demanding more energy and expensive, due to the corrosion of equipment and membrane damage [11]. The use of hydrate technology in the existence of fluorinated refrigerants as a hydrate former shows the improvement in the energy efficiency of desalination processes, because it is essential to produce fresh water from the saline waters at ambient conditions [4,9–22].

* Corresponding authors.
E-mail addresses: amir_h_mohammadi@yahoo.com (A.H. Mohammadi), ramjuger@ukzn.ac.za (D. Ramjugernath).

https://doi.org/10.1016/j.jct.2019.04.012
0021-9614/

Fluorinated hydrate former can play a vital role in water desalination [4,9–22]. The refrigerant has an advantage to form gas hydrate structure with only water. Once hydrate is being formed, the water ideally has zero salinity, that can be achieved by separating residual salinity on the surface of hydrate crystal [6,11–13,19,22]. As a result fresh water would be produced as a desired product of the desalination process when dissociation of gas hydrate takes place. It was revealed, in the study of Ngema *et al.* [11–13], that refrigerants such as R410a, R507 and R134a were capable of forming gas hydrates at pressures underneath 1.2 MPa. Consequently, in order to improve the lower cost of the processes, a hydrate process with low pressure should be utilized [11–13,22–24].

A number of researchers [4,11–13,19,22,25–27] have testified that the utilization of fluorinated hydrate formers for the initiating the formation process of gas hydrates is capable in comparison to conventional processes. A brief review for the formation of a gas hydrate in the addition of a single salt at various concentrations, using a fluorinated refrigerant as hydrate former is compiled and presented in Table 1. It was revealed that the addition of salt to the fluorinated refrigerant + water systems cause the dissociation temperatures to shift to lower values.

While the use of gas hydrates is well established as means of water desalination, no publication of research has been found on the formation of hydrates from water containing mixed electrolytes, using a fluorinated refrigerant and a water insoluble promoter, except for propane (R290) as presented in Table 2. As a result, this study sets out to undertake extensive laboratory measurements of hydrate formation and dissociation data, resulting from the use of two selected fluorinated refrigerants (R410a and R507) on four types of salts (NaCl, $MgCl_2$, $CaCl_2$ and Na_2SO_4) aqueous solutions with and without cyclopentane as a water insoluble promoter.

A thermodynamic promoter is a compound that is used to facilitate hydrate formation by decreasing the required pressure and raise the temperature [3]. Promoters are typically hydrophobic which are classified according to their shape, magnitude and chemical nature [3]. The magnitude of the molecules and type of structure occupied affect the position of the gas within the structure of the hydrate [28]. Hydrate promoters can be distinct as "water soluble" and "water insoluble" [25]. Water soluble promoters can be either thermodynamic or kinetic promoters [3]. Thermodynamic promoters are organic compounds consisting of two types of molecules that alter gas hydrate formation and dissociation condition [3]. The first type of molecule does not take part in the crystal of hydrate cavities [3]. These molecules include THF, acetone, 1,4-dioxane, *etc.* [28]. These molecules typically form structure II in the presence or absence of a help gas molecule [28]. The second type of former molecules, like TBAB, TBAC, TBAF, TBPB, *etc.* takes part in the structuring of cavities in hydrates called semi-clathrate hydrate [28]. A number of researchers [28–36] have investigated the effects of the aforementioned water soluble promoters. For instance, it was found that TBAB changes the structure of cavities while THF does not, but both promoters increase the formation and dissociation temperatures.

Kinetic promoters are typically surfactant molecules, which include sodium dodecyl sulfate (SDS), that affect the speed of hydrate formation [37,38]. An ionic surfactant (SDS) increases hydrate formation rate [39–41]. The use of a surfactant in hydrate formation is an effective method for reducing power consumption. Roosta *et al.* [42] reported on the promotion effect of a surfactant on gas hydrate formation kinetics. Surfactants are used to improve the amount of gas used during the formation of hydrate crystals without affecting the equilibrium conditions [43,44].

The water insoluble thermodynamic promoters typically consist of cyclic hydrocarbons as they are listed in literature [28]. These cyclic hydrocarbons such as methylcyclohexane (MCH), cyclopentane (CP), cyclohexane (CH), *etc.* normally form structure H hydrates (in the presence of a gas called help gas), except for CP and CH that form sII hydrates [3]. Structure H hydrate formers fill the large cages of the hydrate structure [3]. They can be utilized to rise the volume of gas storage in gas hydrates [3,25].

Cyclopentane is chosen to be used as the promoter for the investigated systems, due to the following advantages [1,44–46]:

- It is water immiscible due to its very low solubility in water (that is why it is called water insoluble)
- It does not affect the hydrate structure
- It allows the desalinated water and concentrated brine to be separated easily
- It is environmental friendly and it is not a harmful organic chemicals
- It is easily recovered due to its immiscibility.

Generally, CP forms structure sII hydrate, as mentioned earlier [3]. It has a great potential to stabilise the temperature and pressure conditions to less pressures and elevated temperatures, compared to hydrate formers of sI and sH hydrates [3]. Herslund [47]

Table 1
Brief Review for Gas Hydrate Formation in Single Salt Aqueous Solution at Various Concentrations Using a Fluorinated Refrigerant as Hydrate Former.

Hydrate former	Salt	w_i (mass fraction)	T/K	P/MPa	References
R13	NaCl	0.020–0.050	271.7–279.7	0.305–2.030	[18]
R23	NaCl	0.020–0.050	272.6–290.6	0.344–3.440	[18]
R152a	NaCl	0.020–0.050	271.0–286.6	0.059–0.413	[18]
R290	NaCl	0.020–0.050	271.0–276.6	0.138–0.471	[18]
R290	$CaCl_2$	0.150	268.7–271.7	0.205–0.412	[78]
R22	NaCl	0.050–0.150	274.0–287.3	0.273–0.775	[26]
R22	KCl	0.050–0.150	275.1–287.8	0.199–0.790	[26]
R22	$MgCl_2$	0.050–0.150	273.9–287.4	0.319–0.783	[26]
R290	NaCl	0.050–0.150	271.5–275.1	0.200–0.400	[52]
R290	KCl	0.050–0.150	273.8–278.0	2.010–3.350	[52]
R410a	NaCl	0.050–0.100	276.1–290.9	0.240–1.345	[11]
R410a	$CaCl_2$	0.038–0.060	280.8–291.4	0.315–1.341	[12]
R410a	$MgCl_2$	0.023–0.047	274.9–291.8	0.154–1.343	[13]
R507	NaCl	0.050–0.100	273.9–281.0	0.226–0.802	[11]
R507	$CaCl_2$	0.038–0.060	274.7–282.5	0.191–0.834	[12]
R507	$MgCl_2$	0.023–0.047	274.3–282.0	0.174–0.823	[13]
R134a	NaCl	0.050–0.150	268.1–280.6	0.086–0.383	[11]
R134a	$CaCl_2$	0.038–0.060	276.2–281.2	0.125–0.392	[12]
R134a	$MgCl_2$	0.047–0.070	274.7–282.2	0.116–0.410	[13]
R22	NaCl	0.030–0.180	273.2–290.2	0.089–0.893	[79]

Table 2
Brief Review for Gas Hydrate Formation in Mixed Salt Aqueous Solution at Various Concentrations Using a Fluorinated Refrigerant as Hydrate Former.

Hydrate former	Salt	w_i (mass fraction)	T/K	P/MPa	References
R290	NaCl + KCl	0.075 + 0.075	265.2–269.1	0.157–0.372	[78]
	NaCl + $CaCl_2$	0.075 + 0.075	265.9–269.4	0.172–0.418	[78]
	$CaCl_2$ + KCl	0.075 + 0.075	266.3–270.1	0.181–0.432	[78]
	$CaCl_2$ + NaCl + KCl	0.050 + 0.075 + 0.075			[78]
R290	NaCl + KCl	0.050 + 0.050	270.4–272.4	0.234–0.441	[80]
	NaCl + $CaCl_2$	0.049 + 0.038	270.9–273.5	0.234–0.441	[80]
R290	NaCl + KCl + $CaCl_2$		248.0–278.0	0.100–0.540	[81]

compared the use of promoters, CP (sII) and methyl-cyclohexane (sH), in the presence of methane gas as a help gas. The equilibrium conditions for both systems were shifted to higher temperatures and lower pressures [3]. It was also found that CP has higher effect than the methyl-cyclohexane (sH) [3,47].

However, CP has very low solubility in water under certain situations of hydrate formation, for example, the solubility is 86 $mg{\cdot}L^{-1}$ at 283 K [3]. It forms an organic liquid phase when used an extra quantity [47]. In the case of an extra quantity of CP present in the system, the aqueous phase is always saturated. Herslund [47] revealed that CP solubility in water is limited in relation to its concentration with changing temperature and pressure. Consequently, the gas hydrate stability conditions are dependent on only a small amount of CP because of its limited solubility, a small quantity is available in the aqueous phase [48].

Cha and Seol [19] and Corak *et al.* [20] stated that the formation of a hydrate in the presence of CP might be employed for seawater desalination. Nevertheless, the hydrate formation without a promoter was slow, as was the case with any other hydrate formation. Cha and Seol [19] suggested that either CP or cyclohexane can be added in the CO_2 hydrate systems, in order to raise the temperature required for desalination of seawater with a high concentration of salt, for the production of fresh water.

There is limited information on the use of CP as a promoter in the presence of fluorinated refrigerants [3]. This study explores its potential use in the presence of single salt in a desalination process using gas hydrates technology. The use of a single salt in the presence of fluorinated refrigerants (R410a, R507 and R134a) as hydrate formers without a promoter was investigated by Ngema *et al.* [11–13]. It has been shown that the addition of salt to the mentioned fluorinated refrigerants + water systems shifts the hydrate stability conditions to lower temperatures with an increase in electrolyte concentration. Moreover, it was revealed that these systems show a quadruple point, which is a condition where the four phases coexist [11–13].

The objective of this investigation was to obtain a precise hydrate dissociation data that can be potentially utilized in the design or optimization existing wastewater plant and desalination plant. The gas hydrate measurements {(R410a or R507) + water + (NaCl or $CaCl_2$ or Na_2SO_4)} were undertaken at different salt concentrations in the absence and presence of CP. The ternary systems for {(R410a or R507) + water + CP} were investigated in the temperature and pressure ranges of (279.8 to 294.4) K and (0.158 to 1.385) MPa, respectively. Measurements for {R410a + water + (NaCl or $CaCl_2$) + CP} systems were undertaken at various concentrations of (0.10, 0.15 and 0.20) mass fractions in the temperature and pressure ranges of (278.4–293.7) K and (0.214–1.179) MPa. The temperature and pressure conditions for R410a + water + Na_2SO_4 system were studied at salt concentration of 0.10 mass fraction at (283.3–291.6) K and (0.483–1.373) MPa, respectively. Measurements for {(R410a + R507) + water + mixed electrolytes (NaCl or $CaCl_2$ or $MgCl_2$)} systems were studied at various salt concentrations of (0.002–0.15) mass fractions in the temperature and pressure ranges of (274.5–292.9) K and (0.149–1.119) MPa, respectively, in the absence and presence of CP. The concentrations, temperature and pressure range for single and mixed salts experiments are summarized in Tables 3 and 4, respectively. The non-visual isochoric equilibrium cell in cooperate pressure-search technique was utilized to undertake hydrate dissociation conditions measurements. The measurements were correlated using a combination contribution of Deybe-Huckel [49], van der Waals and Platteeuw [50], and CPA-EoS [51] models. These combinations are formed a new model which is called Hydrate Electrolyte–Cubic Plus Association (HE–CPA). The Deybe-Huckel [49] was used to model the electrolyte aqueous systems and the crystalline solution concept of van der Waals and Platteeuw [50] was employed to model the hydrate phase and the CPA [51] equation of state was used for the liquid or vapour phases.

2. Experimental

2.1. Materials

The purity and the information of the chemicals and suppliers are tabulated in Table 5. A 2010 model gas chromatograph (Shimadzu) equipment with a thermal conductivity detector and a Porapak Q column was utilized to check the purities of the refrigerants (R410a and R507). Mill-Q water which has a conductivity of (5.5555 $\mu S{\cdot}m^{-1}$) at 298.15 K was utilized to prepare aqueous solution for all systems of interest. The gravimetric method was used to prepare (NaCl or $MgCl_2$ or $CaCl_2$ or Na_2SO_4) aqueous solutions. A precise analytical balance, Model AV 114 (Ohaus Adventurer) with a manufacture error of ±0.0001 g in mass was utilized for the synthesis of the electrolyte mixtures. It should be noted that the salt concentrations in this study correspond to the (water + salt) system.

2.2. Apparatus

Fig. 1a shows the cylindrical isochoric equilibrium cell used in this study and it has an approximate volume of 38 cm^{-3}. Fig. 1b shows the agitation device that was used for homogenous mixing of the content in the equilibrium vessel. It is made of neodymium magnets and it is consists of four stainless steel impeller blades as well as Teflon that is use to avoid friction between mechanical shaft and neodymium magnets. Figs. 2a and 2b respectively show a flow diagram of the isochoric cell and the apparatus layout used to undertake gas hydrate measurements. The full details of the equilibrium cell are specified in literature [11,22]. A class A ceramic Pt-100 was utilized to undertake equilibrium temperatures. It was calibrated by immersing in the temperature controlled bath with ethylene glycol solution and a standard WIKA temperature probe connected to a WIKA CTH 6500 multi-meter. The WIKA temperature sensor has a manufacture uncertainty of ±0.03 K. The combined expanded uncertainty in the temperature measurement is estimated to be ±0.03 K (*0.95 level of confidence*). The pressure in the isochoric vessel was undertaken with a WIKA pressure transmitter rated pressure up to 10 MPa. It was calibrated in the pressure range between 0 and 10 MPa against a standard pressure

Table 3
Temperature and Pressure Ranges studied for Hydrate Dissociation Conditions in the Absence and Presence of Cyclopentane (CP) at Various Salt Concentration (w_i = Mass Fraction).

Hydrate systems	Salt	w_i (mass fraction)	No. points	T/K	P/MPa
[a]R410a + water	No salt	–	10	277.5 to 293.0	0.179 to 1.421
R410a + water + CP	No salt	–	7	280.9 to 294.4	0.158 to 1.385
[b]R410a + water	NaCl	0.10	8	276.1 to 288.6	0.240 to 1.271
R410a + water + CP	NaCl	0.10	7	280.2 to 290.5	0.286 to 1.179
R410a + water + CP	NaCl	0.20	7	278.4 to 285.8	0.286 to 0.879
R410a + water + CP	$CaCl_2$	0.10	7	281.5 to 292.3	0.214 to 1.056
R410a + water + CP	$CaCl_2$	0.15	6	279.9 to 289.9	0.217 to 1.004
R410a + water	Na_2SO_4	0.10	7	278.3 to 291.6	0.199 to 1.373
[b]R507 + water	No salt	–	9	277.7 to 283.3	0.221 to 0.873
R507 + water + CP	No salt	–	7	279.8 to 284.6	0.248 to 0.858

[a] Reference [73],
[b] Reference [11]

Table 4
Temperature and Pressure Ranges Studied for Hydrate Dissociation Conditions in the Absence and Presence of CP at Mixed Salt Concentration (w_i = Mass Fraction).

Hydrate systems (w_i = mass fractions)	No. points	T/K	P/MPa
R410a + water + 0.002 $CaCl_2$ + 0.017 NaCl	7	279.6 to 289.1	0.250 to 1.019
R410a + water + 0.002 $CaCl_2$ + 0.017 NaCl + CP	6	283.3 to 292.5	0.299 to 1.119
R410a + water + 0.013 $MgCl_2$ + 0.0193 NaCl	7	282.3 to 292.9	0.238 to 1.169
R410a + water + 0.013 $MgCl_2$ + 0.0193 NaCl + CP	8	279.1 to 288.9	0.244 to 1.018
R507 + water + 0.002 $CaCl_2$ + 0.017 NaCl	9	277.8 to 283.0	0.149 to 0.730
R507 + water + 0.002 $CaCl_2$ + 0.017 NaCl + CP	7	279.5 to 284.1	0.436 to 0.677
R410a + water + 0.08 $CaCl_2$ + 0.05 NaCl	8	276.4 to 288.8	0.246 to 1.067
R410a + water + 0.08 $CaCl_2$ + 0.05 NaCl + CP	7	280.6 to 291.7	0.199 to 1.099
R410a + water + 0.15 $CaCl_2$ + 0.05 NaCl	9	274.5 to 282.1	0.279 to 1.074
R410a + water + 0.15 $CaCl_2$ + 0.05 NaCl + CP	7	278.1 to 289.4	0.204 to 1.041

Table 5
Purities, Critical Properties, and Suppliers Names of the Refrigerant Studied.

Chemicals	Formula	Molar mass/(g·mol^{-1})	Supplier	Purity* (mass fraction)	T_c/K	P_c/MPa	ω
Water	H_2O	18.015[a]	UKZN	1.000	647.14[a]	22.064[a]	0.344[a]
Cyclopentane	C_5H_{10}	70.10	Merck	0.999	511.60[a]	4.508[a]	
R410a	0.5CH_2F_2 + 0.5 CHF_2CF_3[d]	72.60[b]	Afrox	0.998	345.65[b]	4.964[b]	0.279[c]
R507	0.5CHF_2CF_3 + 0.5CH_3CF_3[d]	98.80	Afrox	0.998	343.96[e]	3.797[e]	0.304[f]
Sodium chloride	NaCl	58.44	Merck	0.990			
Calcium chloride	$CaCl_2$	110.98	Merck	0.990			
Sodium sulphate	Na_2SO_4	142.04	Merck	0.990			

[a] Ref. [79],
[b] Reference [72],
[c] Reference [82],
[d] mass fraction,
[e] Reference [71],
[f] Reference [83].
* As stated by the supplier. Checked by GC analysis for the gases and liquids. T_c is the critical temperature, P_c is the critical pressure and ω is the acentric factor.

transducer from WIKA. The combined expanded uncertainty in the pressure measurement is ± 0.0007 MPa (*0.95 level of confidence*).

2.3. Experimental method

Hydrate dissociation data obtained in this study were obtained by applying an isochoric pressure-search method [11–13,22,25,52]. The Mill-Q water was utilized to clean the apparatus. Acetone was utilized to wash the cell, after which the cell was evacuated to 0.2 kPa for a period of 30 min to make sure there were no residue of impurities. A volume of 20 cm^3 of {NaCl or $MgCl_2$ or $CaCl_2$ or Na_2SO_4} aqueous solutions with 10% of the approximately volume of CP was charged into the equilibrium cell. The equilibrium vessel was submerged into fluid bath with Polyscience temperature-controlled and the fluorinated refrigerants were fed from cylinder through a pressure controlled valve into the vessel. The electrolyte solution for {(R410a or R507) + water + (NaCl or $CaCl_2$ or $MgCl_2$ or Na_2SO_4)} systems, either in the absence or presence of CP was given a period of 30 min to allow the gas to be absorbed into the solution until the system stabilised. The equilibrium cell contents were stirred at stirrer speed of 600 rpm [12,13].

It is important to ensure that the system is at equilibrium outside the hydrate stability zone before starting the process. Thereafter, the temperature was programmed to drop gradually in order to allow the hydrate to be formed. During the formation, the pressure slowly reduced as the temperature of the systems decreases slowly. At the point where a drastic drop in pressure is noted, it is a point where the hydrate is being formed. A cycle for the reduction and increase in temperature and pressure is illustrated in Fig. 3a, it is showing gas hydrate formation and dissociation. Once the hydrate is being formed, the system temperature was slowly increased. As the heating curve approaches the dissociation point, the increment step in temperature was set to 0.1 K as shown in Fig. 3b. Once the equilibrium is attained proximity after sixty minutes, the temperature is programmed for s step increase of 0.1 K. At the point where the cycle is formed as illustrated in

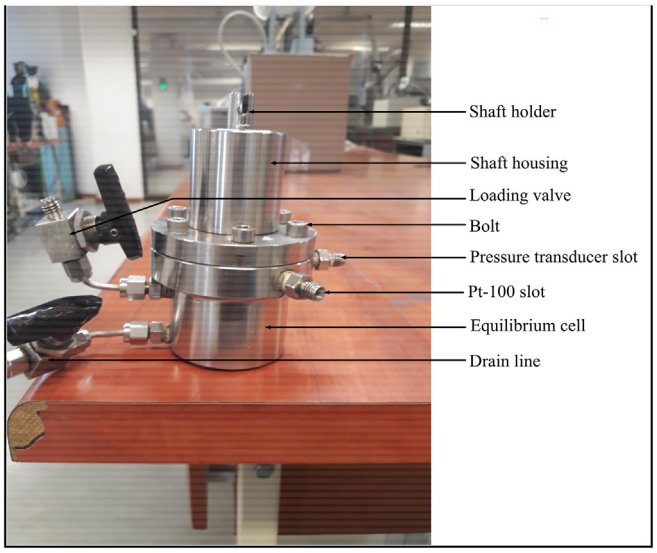

Fig. 1a. The Isochoric Equilibrium Cell.

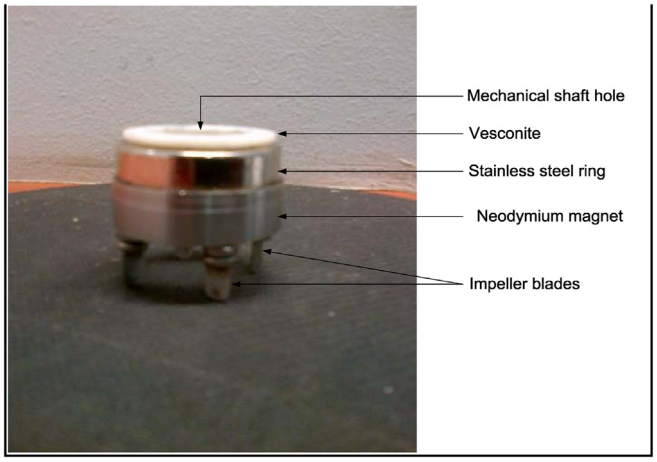

Fig. 1b. Stirring Device Made with Neodymium Magnets.

Fig. 3b, the refrigerant is released. Consequently, the content inside the equilibrium cell goes back to initial stage where the system is stable outside hydrate formation zone. The point where the complete hydrate cycle is formed is called hydrate dissociation point, which is where the hydrate system conditions are at equilibrium.

3. Development of thermodynamic model

In this study, three models were combined into one model, namely, the van der Waals and Platteeuw, Debye–Hückel (DH) and CPA Equation of State (EoS). The combination contributions were developed from electrolyte–CPA (e-CPA) equation of state of Maribo-Mogensen [53], consequently, a developed model namely, Hydrate Electrolyte–Cubic Plus Association equation of state, is introduced which has the following contributions:

$$A^{HE-CPA} = A^{CPA} + A^{DH} + A^{Hydrate} \tag{1}$$

From Eq. (1), the model of van der Waals and Platteeuw [50] is use to model the hydrate phase. This model was amended by Eslamimanesh *et al.* [25], which was used in this study, the electrolytes aqueous systems are modeled using Deybe–Hückel [49], and CPA [51] equation of state model is used for liquid or vapour phase. A computational algorithm diagram for the HE–CPA is presented in Fig. 4.

3.1. The Cubic-Plus-Association equation of state

For any system at equilibrium, the chemical potential of each component in all coexisting phases are equal. The fugacity of component in the liquid phases was calculated using the CPA EoS that employs the combination of Soave-Redlich-Kwong (SRK) [54] EoS and association term. The CPA EoS was developed by Kontogeorgis *et al.* [51], which is widely used in petroleum industry to describe the complex solution comprising hydrocarbons and polar/association chemicals, including water, alcohols, organic acids, *etc.* [55]. The CPA EoS provides the following advantages [55]:

- It gives accurate results for multicomponent evaluation using only the parameters predicted from binary data;
- It uses a scientific formulation, but with a contextual to described complex mixtures;
- It reduces the classical SRK EoS as it provides a representation of hydrocarbon phase equilibria. SRK is considered as an acceptable and effective to calculate the cubic EoS of petroleum fluids.

This is used to describe the physical interactions which can be employed to different types of hydrogen bonding compounds such as water [56,57]. The studied systems in the present work contain water as key component that has self-association [58], consequently, in this study, water is the only associating component. The water parameters are determined from pure liquid water properties. Table 6 presents the CPA cross-association energy and volume parameters for water that are used for the fugacity calculations. It also presents the energy parameter of the equation of state given by a Soave [54] type temperature dependency, while b is temperature independent.

$$a(T) = a_o\left[1 + c_1\left(1 - \sqrt{\frac{T}{T_c}}\right)\right]^2 \tag{2}$$

$$a_o = 0.42747\frac{R^2T_c^2}{P_c} \tag{3}$$

$$b = 0.08664\frac{RT_c}{P_c} \tag{4}$$

$$c_1 = 0.480 + 1.574\omega_i - 0.176\omega_i^2 \tag{5}$$

Kontogeorgis *et al.* [51,58] proposed the following expression for CPA EoS:

$$P = \frac{RT}{V_m - b} - \frac{a(T)}{V_m(V_m + b)} - \frac{1}{2}\frac{RT}{V_m}\left(1 + \rho\frac{\partial \ln g}{\partial \rho}\right)\sum_i x_i \sum_{A_i}(1 - X_{A_i}) \tag{6}$$

where ρ represents the molar density, V_m represents the molar volume, X_{A_i} represents the association term, and x_i is the mole fraction.

$$X_{A_i} = \frac{1}{1 + \frac{1}{V_m}\sum_j x_j \sum_{B_j} X_{B_j}\Delta^{A_iB_j}} \tag{7}$$

$$\rho\frac{\partial \ln g}{\partial \rho} = \frac{1.9\eta}{1 - 1.9\eta} \tag{8}$$

where $\Delta^{A_iB_j}$ is the association strength and it can be determined by:

$$\Delta^{A_iB_j} = g(\rho)\left[\exp\left(\frac{\varepsilon^{A_iB_j}}{RT}\right) - 1\right]b_{ij}\beta^{A_iB_j} \tag{9}$$

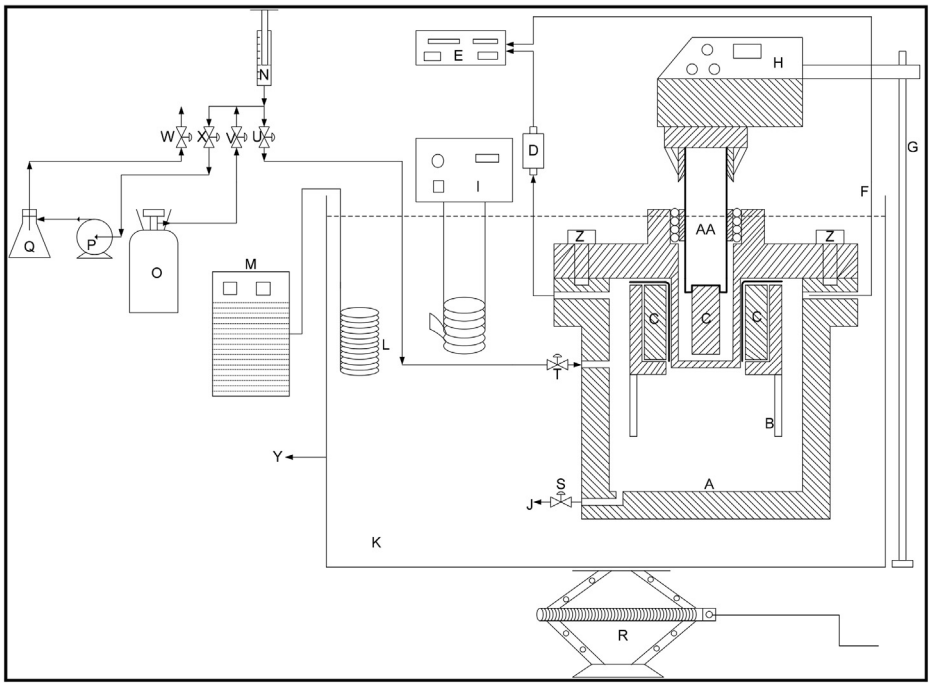

Fig. 2a. Schematic Flow Diagram for Isochoric Pressure Equilibrium Cell, [13]: A, Isochoric cell; B, Impeller; C, Neodymium magnet; D, Pressure transducer; E, Data acquisition unit; F, Pt-100; G, Stainless steel stand; H, Overhead mechanical stirrer; I, Temperature programmable circulator; J, Drain line; K, Chilling fluid; L, Cooling coil; M, Cold finger; N, Liquid syringe with aqueous solution; O, Refrigerant gas cylinder; P, Vacuum pump; Q, Vacuum flask; R, Mechanical jack; S, Drain valve; T, Inlet valve; U, Loading valve; V, Gas valve, W, Vent valve to atmosphere; X, Vacuum valve; Y, Water bath and Z, Stainless steel bolts; AA, Mechanical shaft.

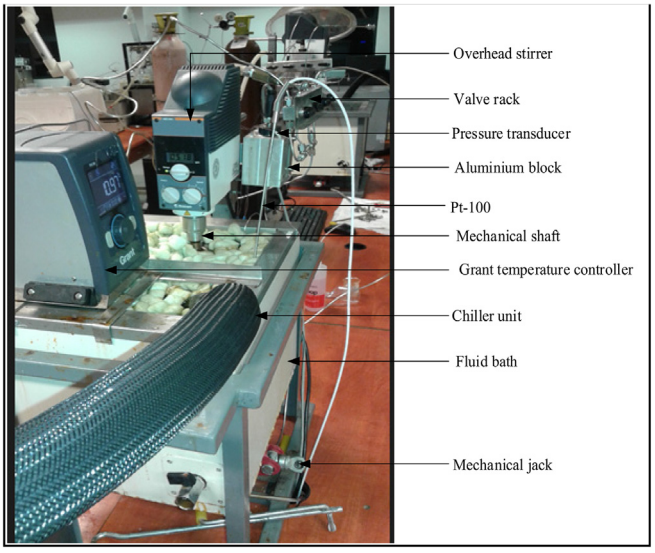

Fig. 2b. A Layout of the Equipment.

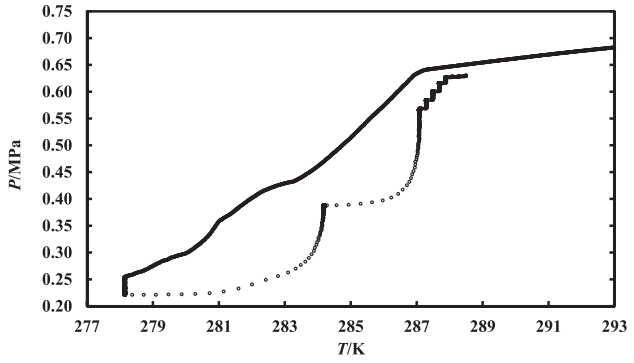

Fig. 3a. Typical Formation and Dissociation Hydrate Curves for the Refrigerant (1) + Water (2) System.

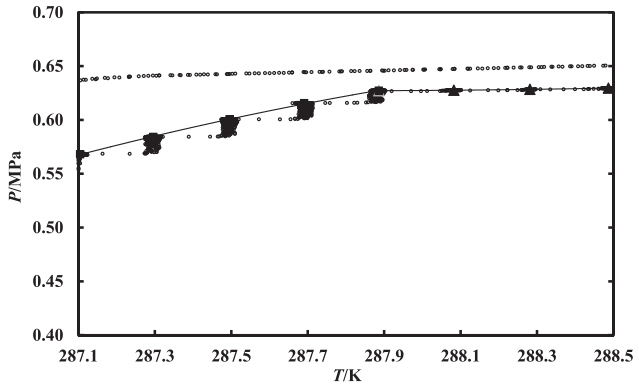

Fig. 3b. Typical Analysis for the Determination of Hydrate Dissociation Point for the Refrigerant (1) + Water (2) System.

where $g(\rho)$ is the radial distribution function, ϵ^{AiBi} represents the cross-association energy, β^{AiBi} stands for the cross-association volume parameter, b_{ij} is the cross parameter obtained from SRK EoS, R represents the Universal gas constant in J.mol^{-1}.K^{-1}, and T is the temperature in Kelvin.

The association strength of CPA is reliable on the best of association scheme. Table 7 presents the quantity and type of association sites for the compound. According to Haghighi *et al.* [59], the association scheme and the quantity of association sites can be determined by checking, at the location, its constituting hydrogen atoms and lone pairs on proton acceptor atoms. Huang and Radosz [60] identified eight different association schemes as

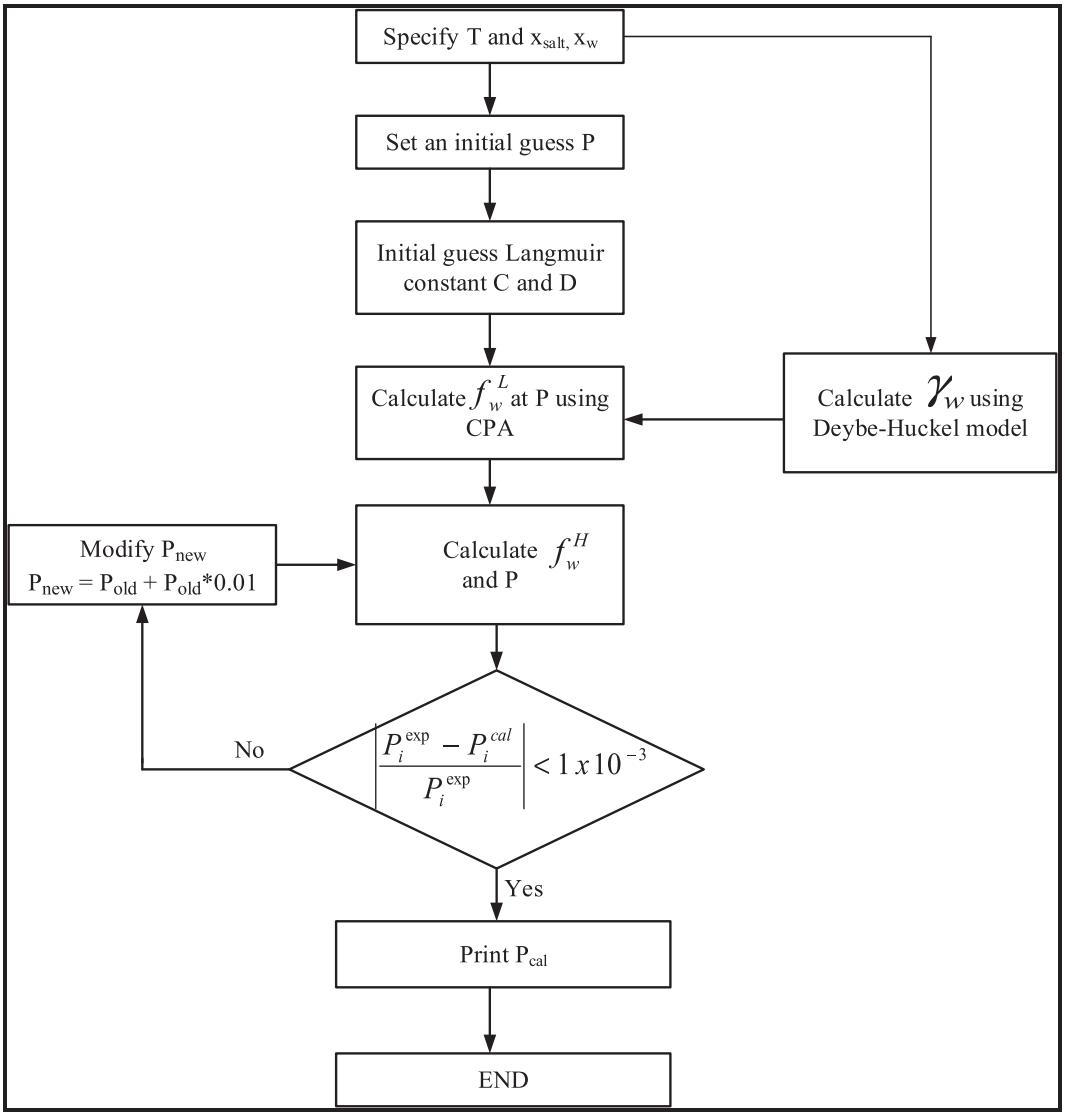

Fig. 4. Computational Flow Diagram.

Table 6
CPA Parameters for Associating Compound (Pure Water) [55,56,58].

Compound	b/(L·mol^{-1})	a_0/(bar·L^2·mol^{-2})	c_1	ε/bar·L·mol^{-1})	β
Water	1.4515	0.12277	0.6736	16,655	69,200

b is the co-volume, a_0 and c_1 are the parameters in the energy term, ε is the association strength and β is the association volume parameter; 1 bar = 100 kPa..

presented in Table 7. These association schemes can be used in different molecules depending on the number and type of associating sites.

In Table 7, the one site (1A) scheme is used for acids, based on the assumption that the site performs as a glue spot. The site is capable to bond with a lone pair electron of an H atom or a site of the similar type. The two-site (2B) or three site (3B) schemes can be employed for alcohols and amines. In the 3B formalism for alcohol, sites A and B match to oxygen lone pairs, whereas site C corresponds to an H atom.

Due to the asymmetry of the association, the fraction of non-bonded H atoms (X_C) is not equal to the fraction of non-bonded lone pairs (X_A or X_B). In the 2B formalism, the two lone pairs for oxygen are taken as a single site [56,57]. The four-site (4C) association scheme is utilized for hydrogen-bonded compounds, such as water and glycols. These compounds have two proton donors and two proton acceptors [56,57].

The selection of association scheme is based on the key component. In this study, water is a key component of all investigated systems. Consequently, the four-site (4C) association scheme was selected to be used as it is traditionally used for water within the CPA framework [58,61–64]. In the 4C formalism, the bonding arrangement means that all non-bonded site fractions are equal [64].

The fugacity coefficient, ϕ_i,can be determined by using Eq. (10):

$$RT\ln\varphi_i = \left(\frac{\partial A^r}{\partial n_i}\right)_{T,V,n_j} - RT\ln Z \tag{10}$$

Table 7
Schematic of Association Schemes [60].

Species	Formula	Type	Site fraction (X)
Acids	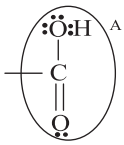	1A	$X_1 = X_A$
Alcohols	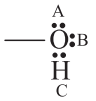	3B	$X_A = X_B$; $X_C = 2X_A - 1$ $X_1 = X_A X_B X_C$
	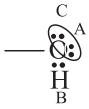	2B	$X_A = X_B$ $X_1 = X_A X_B$
Glycols	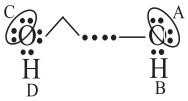	4C	$X_A = X_B = X_C = X_D$ $X_1 = X_A X_B X_C X_D$
Water	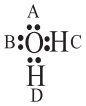	4C	$X_A = X_B = X_C = X_D$ $X_1 = X_A X_B X_C X_D$
		3B	$X_A = X_B$; $X_C = 2X_A - 1$ $X_1 = X_A X_B X_C$
		3B[a]	$X_A = X_B$; $X_C = 2X_A - 1$ $X_1 = X_A X_B X_C$
		2B	$X_A = X_B$ $X_1 = X_A X_B$

[a] Assuming one proton donor and two proton acceptors for water results in the same mathematical expression as if two proton donors and one proton acceptor

where A^r represent the remaining Helmholtz energy for the solution.

$$Z = \frac{PV}{nRT} \tag{11}$$

The CPA EoS is the combination of SRK EoS and the association term, as mentioned earlier:

$$A^r(T,P,n) = A^r_{SRK}(T,P,n) + A^r_{ass}(T,P,n) \tag{12}$$

The fugacity coefficient for the SRK term can be determined using Eq. (13) [65]:

$$\frac{A^r_{SRK}(T,P,n)}{RT} = -n\ln\left(1 - \frac{B}{V}\right) - \frac{D(T)}{RTB}\ln\left(1 + \frac{B}{V}\right) \tag{13}$$

where V represents the total volume of the system. According to Michelsen and Mollerup [65], $D(T)$is used instead of $\alpha(T)$ for consistency. The detail on how to calculate term B is found elsewhere in literature [55,65]

Thus, the fugacity from CPA is:

$$f_i^{\alpha} = x_i \phi_i^{SRK} P \tag{14}$$

where αcan be a vapour or liquid.

3.2. Electrolyte model

In the presence of electrolyte, the activity coefficient in the aqueous solution is calculated using the Debye–Hückel model. Electrolyte thermodynamic models describe different contributions to excess Gibbs energy. Normally, they consist of explicit terms to take into account short-range, intermediate-range and long-range interactions in the specified solution, as presented in the following expression:

$$G^E = G^{SR} + G^{MR} + G^{LR} \tag{15}$$

Table 8 presents common activity coefficient models used in chemical and wastewater industries [66]. These models are based on extension of a local composition term (modified NRTL or UNIQUAC) with an additional model to take the electrolytes into account. Lin *et al.* [66] reported that these models require a large number of interaction parameters to be estimated against the existing experimental data. These parameters, in general, are not transferable outside the regime where they are estimated.

The Deybe–Hückel is the initial point for the development of activity coefficient models for electrolyte solutions, which was developed in 1923 by P. Deybe and E. Hückel. It is considered as an exact equation to describe the behaviour of an electrolyte system at infinite dilution [67]. The following assumptions were made by Gmehling *et al.* [67] for the derivation of the Deybe–Hückel limiting law:

- Only the electrostatic forces between the ions are considered and all the other forces are negligible;
- The electrostatic interactions are small compared to the thermal energies;
- The ions are considered as punctual charges with a spherical field;
- The dielectric constant of the solution is equal to that of the solvent;
- The electrolyte is completely dissociated;
- Each ion is surrounded by ions of an opposite charge;
- Solutions of electrolyte(s) are diluted to lower concentrations;
- The distribution of ions around a center ion is controlled by Boltzmann's law because of existing electric potential.

Table 8
Activity Coefficient Models for Electrolyte Solutions and their Applications [53].

Model	Electrolyte NRTL[a,b]	OLI mixed solvent electrolyte[e,f,g,h,i]	Extended UNIQUAC[l,m,n]
Non-electrostatic term	Modified NRTL[a]	UNIQUAC[j] + 2nd virial term[k]	UNIQUAC[j]
Electrostatic term	Modified Pitzer-Debye–Hückel[b,c] and Born[d]	Modified Pitzer-Debye–Hückel[c,e]	Extended-Debye–Hückel[o]
Parameters	2–4 per binary (on ion pair basis)	3 per binary	4 per molecule, 2 per binary
Availability	Aspen Plus/ Properties	Aspen Plus/ HYSYS, Honeywell UniSim, gPROMS, Pro/II	Aspen Plus and Excel

[a] Reference [83],
[b] Reference [84],
[c] Reference [85],
[d] Reference [86],
[e] Reference [87],
[f] Reference [88],
[g] Reference [89],
[h] Reference [90],
[i] Reference [91],
[j] Reference [92],
[k] Reference [93],
[l] Reference [68],
[m] Reference [94],
[n] Reference [95],
[o] Reference [49]

Lin *et al.* [66] compared the activity coefficient models listed in Table 6 by conducting ten test systems. These systems include an aqueous mixture with salts (NaCl, Na_2SO_4, $MgCl_2$, KNO_3, K_2SO_4, $MgSO_4$, $MgNO_3$) and a mixed solvent system with water and ethanol. From Table 6, the Extended UNIQUAC gives good results in the case of mixed solvent solutions, even at higher concentrations, despite the Debye–Hückel assumption that the solvent is pure water and it does not include the Born term for the Gibbs energy transfer. It was also found that the interaction parameters of the UNIQUAC model can be employed to compensate for the alternative representation of electrostatic interactions. But there was a query about whether the correlation models could produce accurate predictions in regions with limited data, which include high temperature or pressure [66]. In such cases, the fundamental of thermodynamic modelling of electrolyte aqueous solutions is required.

Long range interactions are taken into account by using the Deybe–Hückel model for the electrostatic interactions between charged ions in aqueous electrolytes systems. It describes the thermodynamics of ideal solutions of ions. The interactions between ions and water are not described by the Deybe–Hückel model [68].

The activity coefficient of ion is calculated by a Deybe–Hückel, which is derived from the total Gibbs excess function by molar differentiation:

$$\left[\frac{\partial\left(nG^{E}_{DH}/RT\right)}{\partial n_i}\right]_{T,P,nj,j\neq i} = -Z_i^2\frac{A\sqrt{I}}{1+Ba\sqrt{I}} \tag{16}$$

$$\ln\gamma_i^{DH} = -Z_i^2\frac{A\sqrt{I}}{1+Ba\sqrt{I}} \tag{17}$$

where A is the Deybe–Hückel parameter:

$$A = (2\pi N_A\rho_0)^{1/2}\left(\frac{e^2}{\varepsilon_0\varepsilon_r kT}\right)^{32} \tag{18}$$

where e is the electronic charge; $\varepsilon_0$is the permittivity in vacuum; $\varepsilon_r$is the dielectric constant or relative permittivity of the solvent, N_A is Avogadro's number, $\rho_0$is molar density, k is the Stefan-Boltzmanns constant and T is the temperature in Kelvin. The value of the Deybe–Hückel parameter A is 1.1717 $(kg/mol)^{1/2}$ at 298.15 K [68] and it can be approximated in the temperature range (273.15–383.15) K by Eq. (19)

$$A = 1.131 + 1.335*10^{-3}(T-237.15) + 1.164 *10^{-5}(T-273.15)^2 \tag{19}$$

In Eq. (17), a is a common ion size parameter replacing the individual distance of closest approach, a_i. The ion size parameter, a, is within the range of 3.5–6.2 × 10^{-10} m [67,68].

Lewis and Randall [69] introduced the concept of ionic strength in Eq. (17),

$$I = 0.5\sum_i m_i Z_i^2 \tag{20}$$

where m_i is the molality (mol.kg^{-1}); and Z is the charge component:

Parameter B in Eq. (17), is determined by the following expression:

$$B = \left(\frac{2e^2N_A\rho_o}{\varepsilon_0\varepsilon_r kT}\right)^{1/2} \tag{21}$$

3.3. Hydrate phase model

The hydrate phase is modeled using the van der Waals and Platteeuw [50] model that was adapted by Parrish and Prausnitz [70]. In 2011, this model was developed by Eslamimanesh *et al.* [25]. In the present study, the amended model of Eslamimanesh *et al.* [25] was selected to be used to model the hydrate phase. This model is well described in details in literature [2,3,11,22,25]. In this model, the fugacity of water in the liquid/aqueous phase, $\left(f_w^L\right)$is equal to the fugacity of water in the hydrate phase$\left(f_w^H\right)$.

$$f_w^H = f_w^{MT}\exp\frac{\mu_w^H-\mu_w^{MT}}{RT} \tag{22}$$

where f_w^{MT}represents the fugacity of water in the empty hydrate phase, μ_w^Handμ_w^{MT} represent the chemical potential of water in the filled and empty hydrate, respectively. R and T represent the universal gas constant and temperature in Kelvin. The crystalline solution concept [50] can be employed to determine the exponential term in Eq. (22).

$$\frac{\mu_w^H-\mu_w^{MT}}{RT} = -\sum_i \nu_i'\ln\left(1+\sum_j C_{ij}f_i\right) = \sum_i \ln\left(1+\sum_j C_{ij}f_j\right)^{-\nu_i'} \tag{23}$$

where ν_i'represents the quantity of cavities of type i per water molecule, C_{ij} represents the Langmuir constant parameter for the interaction for guest molecule and f_j represents the fugacity of guest molecule [2,3,11,22,25]. Consequently, the fugacity of water in the empty hydrate phase in Eq. (22) can be calculated by the following expression:

$$f_w^{MT} = P_w^{MT}\phi_w^{MT}\exp\int_{P_w^{MT}}^{P}\frac{v_w^{MT}dP}{RT} \tag{24}$$

where ν_i' represents the vapour pressure of the empty hydrate cage, φ_w^{MT}represents the correction factor from ideal behaviour, and v_w^{MT} represents the partial molar volume of water in the empty hydrate. The exponential term is the Poynting correction. Eslamimanesh *et al.* [25] made two assumptions, and Eq. (24) can be rewritten as [2,3,22,25]

$$f_w^{MT} = P_w^{MT}\exp\left[\frac{v_w^{MT}\left(P-P_w^{MT}\right)}{RT}\right] \tag{25}$$

By substitution of Eq. (25) into Eq. (22), the fugacity of water in the hydrate phase is expressed by:

$$f_w^H = P_w^{MT}\exp\left[\frac{v_w^{MT}\left(P-P_w^{MT}\right)}{RT}\right]\left[\left(1+C_{small}f_{gas}^V\right)^{-\nu'_{small}}+\left(1+C_{large}f_{gast}^V\right)^{-\nu'_{large}}\right] \tag{26}$$

where f_{gas}^V represents the fugacity of hydrate former or refrigerant in the vapour phase that can be determined by using CPA equation of state. In this study, the Poynting correction term is negligible due to dissociation pressures are not very high [25]. Sloan and Koh [3] described the equations that can be used to calculate p_w^{MT}, and, ν_i' for sI and sII [2,3,22,25]:

for structure I

$$P_w^{MT} = 0.1\exp\left(17.440-\frac{6003.9}{T}\right) \tag{27}$$

ν'_{small} = 1/23
ν'_{large} = 3/23
for structure II

$$P_w^{MT} = 0.1\exp\left(17.332-\frac{6017.6}{T}\right) \tag{28}$$

v'_{small} = 2/17
v'_{large} = 1/17
where p_w^{MT} is in MPa and T is in Kelvin

Langmuir constants are accountable for the interactions among the refrigerants and water molecules in the cavities, as stated by Parrish and Prausnitz [70], for a certain hydrate former evaluated over a certain range of temperatures [25]. In the model of Eslamimanesh *et al.* [25] the model parameters are determined by using the equation of Parrish and Prausnitz [70].

For a small cavity (pentagonal dodecahedral)

$$C_{small} = \frac{a}{T}\exp\left(\frac{b}{T}\right) \tag{29}$$

and for a large cavity (tetrakaidecahedra (sI) and hexakaidecahedra (sII))

$$C_{large} = \frac{c}{T}\exp\left(\frac{d}{T}\right) \tag{30}$$

where T is the temperature in K, C has units of reciprocal MPa and a', b', c', d' are the adjustable parameters for the Langmuir constant.

The value of v_W^{MT} can be obtained using the following equation [25]:

For structure I:

$$v_W^{MT} = \left(11.835 + 2.217\times10^{-5}T + 2.242\times10^{-6}T^2\right)\frac{10^{-30}N_A}{N_W^{MT}} - 8.006\times10^{-9}P + 5.448\times10^{-12}P^2 \tag{31}$$

For structure II:

$$v_W^{MT} = \left(17.13 + 2.249\times10^{-4}T + 2.013\times10^{-6}T^2 + 1.009\times10^{-9}T^3\right)\frac{10^{-30}N_A}{N_W^{MT}} - 8.006\times10^{-9}P + 5.448\times10^{-12}P^2 \tag{32}$$

where N_A is Avogadro's number and N_W^{MT} represents the number of water molecules per hydrate cell. P and T represent the pressure and the temperature, respectively.

We assumed that structure II is formed for the hydrate systems studied in this work.

The optimum values of the parameters of a Langmuir constant correlation (c' and d') are estimated by tuning the thermodynamic model against the measured data obtained in the literature.

4. Results and discussion

The vapour pressures of fluorinated refrigerant (R410a or R507) were determined by Ngema *et al.* [11] to confirm the Pt-100 and pressure transmitter calibrations and operating procedure for the apparatus. The results agree very well with the one presented in the literature [71,72]. In 2014, Ngema *et al.* [11] conducted the test systems for {(R410a or R134a) + water} and the measured systems strongly agreed with the data presented in literature [73]. This system was conducted to validate the consistency of the apparatus and the technique used to generate accurate and consistent data. Fig. 5 represents the measured hydrate dissociation data for the (R134a + water) system, these data are used later to test the HE–CPA model.

Previous studies of Ngema *et al.* [11–13] indicated that the water insoluble promoter either cyclopentane or cyclohexane is required for the {(R410a or R507) + water + (NaCl or $CaCl_2$)} systems in order to increase hydrate dissociation temperatures near to ambient conditions. Although, it was stated that the (R410a + water) system was forming hydrates near to ambient temperatures. Consequently, in this study, the CP was selected to be used for the {(R410a or R507) + water + (NaCl or $CaCl_2$)} systems to raise the hydrate dissociation temperatures close to ambient conditions.

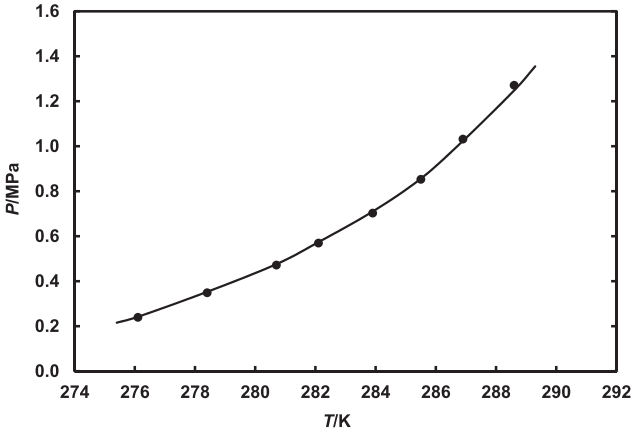

Fig. 5. Experimental and Estimated Hydrate Dissociation Conditions for the R134a (1) + Water (2) Test System: Symbols Represent Experimental Data: ●, Liang *et al.* [96]; ▬, Model Results.

In this study, the hydrate dissociation conditions measurements for {(R410a or R507) + water + single and mixed electrolytes (NaCl, $CaCl_2$, $MgCl_2$ and Na_2SO_4)} systems were undertaken at various salt concentrations in the absence and presence of CP as presented in Tables 9–14 and shown in Figs. 6–15. Hydrate dissociation data for {(R410a or R507) + water + mixed electrolytes (NaCl, $CaCl_2$ and $MgCl_2$)} systems were measured at maximum concentrations of electrolytes at a typical industrial wastewater treatment plant such as Tutuka Eskom, Sasol Secunda and Oil field brine [74–76] as well as at higher concentrations up to 0.15 mass fraction. The selected maximum concentration for industrial wastewater covers the maximum electrolyte concentrations in seawater.

4.1. Effect of cyclopentane

Experimental results indicate that the addition of electrolytes has an inhibiting effect to shift the hydrate phase equilibrium boundary to slightly lower temperatures, but in the presence of CP the R410a systems are closed to ambient temperatures. Consequently, CP makes an impressive increase of hydrate dissociation temperatures for R410a systems with electrolyte.

The results presented in Fig. 6 for the (R410a + water + CP) system show that by the addition of CP the dissociation temperatures increase by 2.4 K compared to the system without CP. For (R410a + water + 0.10 mass fraction of NaCl + CP) system, it can be observed that the hydrate dissociation temperatures increase by 2.7 K compared to the same system in the absence of CP that was measured by Ngema *et al.* [11] as shown in Fig. 7. The {R410a + water + (0.10 and 0.15) mass fraction of $CaCl_2$ + CP} and R410a + water + 0.10 R410a + water + 0.10 mass fraction of Na_2SO_4} systems are showing inhibition effects by shifting hydrate phase equilibrium boundaries to lower hydrate dissociation temperatures as shown in Figs. 8 and 9, respectively.

The results for the (R507 + water + CP) system show an increase in hydrate dissociation temperature by 1.3 K when compared to the (R507 + water) system measured by Ngema *et al.* [11] in the absence of CP as shown in Fig. 10. However, the (R507 + water) system measured by Ngema *et al.* [11] shows the hydrate dissociation temperatures lower than ambient temperature, in this study, it was found that the hydrate dissociation temperatures for this system are lower than ambient temperature even in the presence of

Table 9
Experimental H–L_w–L_p –V (Hydrate – Aqueous Rich – Organic Rich – Vapour) Hydrate Dissociation Conditions for the R410a (1) + Water (2) + NaCl (3) + CP (4) System at Various Salt Concentrations.[a]

R410a (1) + water (2) + CP (3)				R410a (1) + water (2) + 0.10[b] NaCl (3)				R410a (1) + water (2) + 0.10[b] NaCl (3) + CP (4)				R410a (1) + water (2) + 0.20[b] NaCl (3) + CP (4)			
T/K	P^{exp}/MPa	P^{cal}/MPa	AD	T/K	P^{exp}/MPa	P^{cal}/MPa	AD	T/K	P^{exp}/MPa	P^{cal}/MPa	AD	T/K	P^{exp}/MPa	P^{cal}/MPa	AD
294.4	1.385	1.372	0.009	288.6	1.271	1.272	0.001	290.5	1.179	1.172	0.006	285.8	0.879	0.867	0.014
293.7	1.187	1.178	0.008	286.9	1.032	1.036	0.016	289.6	1.041	1.035	0.006	285.2	0.792	0.785	0.009
292.6	0.997	0.991	0.006	285.5	0.853	0.859	0.007	288.6	0.901	0.903	0.002	284.1	0.676	0.676	0.000
290.3	0.742	0.749	0.009	283.9	0.703	0.696	0.010	287.4	0.767	0.761	0.008	283.1	0.587	0.581	0.010
287.0	0.469	0.475	0.013	282.1	0.57	0.559	0.019	286.0	0.633	0.628	0.008	281.5	0.476	0.469	0.015
283.8	0.271	0.275	0.015	280.7	0.472	0.469	0.006	283.2	0.444	0.441	0.007	280.1	0.386	0.383	0.008
280.9	0.158	0.160	0.013	278.4	0.349	0.344	0.014	280.2	0.286	0.283	0.010	278.4	0.286	0.282	0.014
				276.1	0.24	0.238	0.008								

$AD = \frac{|p_i^{cal} - p_i^{exp}|}{p_i^{exp}}$, P–represents the experimental and calculated pressure in MPa.

[a] U(T) (0.95 level of confidence) = 0.1 K, U(P) (0.95 level of confidence) = 0.007 MPa, U(w_i = mass fraction of salt) (0.95 level of confidence) = 0.0002 g. A precise analytical balance, model No. AV 114 (Ohaus Adventurer) with a manufacture error of ± 0.0001 g in mass was utilized for the synthesis of the electrolyte mixtures. It should be noted that the salt concentrations in this study correspond to the (water + salt) system and the R410a is measured as a gas.
[b] Values are in mass fraction for water + salt.

Table 10
Experimental H–L_w–L_p –V (Hydrate – Aqueous Rich – Organic Rich – Vapour) Hydrate Dissociation Conditions for the R410a (1) + Water (2) + $CaCl_2$ (3) + CP (4) System at Various Salt Concentrations.[a]

[b]R410a (1) + water (2)				R410a (1) + water (2) + CP (3)				R410a (1) + water (2) + 0.10[c] $CaCl_2$ (3) + CP (4)				R410a (1) + water (2) + 0.15[c] $CaCl_2$ (3) + CP (4)			
T/K	P^{exp}/MPa	P^{cal}/MPa	AD	T/K	P^{exp}/MPa	P^{cal}/MPa	AD	T/K	P^{exp}/MPa	P^{cal}/MPa	AD	T/K	P^{exp}/MPa	P^{cal}/MPa	AD
293.0	1.421	1.426	0.015	294.4	1.385	1.372	0.009	292.3	1.056	1.049	0.007	289.9	1.004	0.998	0.006
291.3	1.185	1.175	0.008	293.7	1.187	1.178	0.008	290.7	0.835	0.841	0.007	288.1	0.795	0.793	0.003
290.3	1.034	1.026	0.008	292.6	0.997	0.991	0.006	290.0	0.777	0.774	0.004	285.8	0.614	0.602	0.020
289.0	0.868	0.865	0.003	290.3	0.742	0.749	0.009	287.6	0.587	0.583	0.007	283.4	0.413	0.414	0.002
287.8	0.741	0.745	0.005	287.0	0.469	0.475	0.013	284.9	0.385	0.382	0.008	279.9	0.217	0.213	0.018
286.0	0.582	0.590	0.014	283.8	0.271	0.275	0.015	281.5	0.214	0.219	0.023				
284.6	0.484	0.490	0.012	280.9	0.158	0.160	0.013	292.3							
283.1	0.396	0.393	0.008												
280.3	0.257	0.260	0.012												
277.5	0.179	0.180	0.006												

$AD = \frac{|p_i^{cal} - p_i^{exp}|}{p_i^{exp}}$, P–represents the experimental and calculated pressure in MPa.

[a] U(T) (0.95 level of confidence) = 0.1 K, U(P) (0.95 level of confidence) = 0.007 MPa, U(w_i = mass fraction of salt) (0.95 level of confidence) = 0.0002 g. A precise analytical balance, model No. AV 114 (Ohaus Adventurer) with a manufacture error of ±0.0001 g in mass was utilized for the synthesis of the electrolyte mixtures. It should be noted that the salt concentrations in this study correspond to the (water + salt) system and the R410a is measured as a gas.
[b] Reference [11],
[c] Values are in mass fraction for water + salt.

Table 11
Experimental H–L_w–L_p –V (Hydrate – Aqueous Rich – Organic Rich – Vapour) Hydrate Dissociation Conditions for R410a (1) + Water (2) + Na_2SO_4 (3) System at Various Concentrations of Salt.[a]

[b]R410a (1) + water (2)				R410a (1) + water (2) + 0.100[c] Na_2SO_4 (3)				[d]R134a (1) + water (2)			
T/K	P^{exp}/MPa	P^{cal}/MPa	AD	T/K	P^{exp}/MPa	P^{cal}/MPa	AD	T/K	P^{exp}/MPa	P^{cal}/MPa	AD
293.0	1.421	1.426	0.015	291.6	1.373	1.359	0.010	288.6	1.271	1.248	0.018
291.3	1.185	1.175	0.008	289.6	1.067	1.063	0.004	286.9	1.032	1.024	0.008
290.3	1.034	1.026	0.008	288.2	0.901	0.905	0.004	285.5	0.853	0.856	0.004
289.0	0.868	0.865	0.003	285.4	0.627	0.632	0.008	283.9	0.703	0.710	0.010
287.8	0.741	0.745	0.005	283.3	0.463	0.464	0.013	282.1	0.570	0.574	0.007
286.0	0.582	0.590	0.014	281.0	0.316	0.320	0.013	280.7	0.472	0.476	0.008
284.6	0.484	0.490	0.012	278.3	0.199	0.202	0.015	278.4	0.349	0.353	0.011
283.1	0.396	0.393	0.008					276.1	0.240	0.242	0.008
280.3	0.257	0.260	0.012								
277.5	0.179	0.180	0.006								

$AD = \frac{|p_i^{cal} - p_i^{exp}|}{p_i^{exp}}$, P–represents the experimental and calculated pressure in MPa.

[a] U(T) (0.95 level of confidence) = 0.1, U(P) (0.95 level of confidence) = 0.007 MPa, U(w_i = mass fraction of salt) (0.95 level of confidence) = 0.0002 g. A precise analytical balance, model No. AV 114 (Ohaus Adventurer) with a manufacture error of ±0.0001 g in mass was utilized for the synthesis of the electrolyte mixtures. It should be noted that the salt concentrations in this study correspond to the (water + salt) system and the R410a is measured as a gas.
[b] Reference [11],
[c] Values are in mass fraction for water + salt,
[d] Reference [96],

Table 12
Experimental H–L_w–L_p–V (Hydrate – Aqueous Rich – Organic Rich – Vapour) Hydrate Dissociation Conditions for the R507 (1) + Water (2) + Salts (3) + CP (4) System at Industrial Salt Concentrations.[a]

[b]R507 (1) + water (2)				R507 (1) + water (2) + CP (3)				R507 (1) + water (2) + 0.002[c] $CaCl_2$ (3) + 0.017[c] NaCl (4)				R507 (1) + water (2) + 0.002[c] $CaCl_2$ (3) + 0.017[c] NaCl (4) + CP (5)			
T/K	P^{exp}/MPa	P^{cal}/MPa	*AD*	*T*/K	P^{exp}/MPa	P^{cal}/MPa	*AD*	*T*/K	P^{exp}/MPa	P^{cal}/MPa	*AD*	*T*/K	P^{exp}/MPa	P^{cal}/MPa	*AD*
283.7	0.873	0.864	0.010	284.6	0.858	0.845	0.010	283.2	0.831	0.823	0.010	284.0	0.778	0.775	0.005
283.2	0.740	0.733	0.009	284.2	0.744	0.736	0.011	282.9	0.759	0.750	0.012	284.0	0.776	0.773	0.010
282.5	0.611	0.607	0.007	283.6	0.604	0.609	0.008	282.4	0.678	0.671	0.010	283.4	0.667	0.661	0.009
281.6	0.504	0.506	0.004	282.6	0.474	0.476	0.004	282.3	0.670	0.663	0.010	282.5	0.537	0.539	0.004
281	0.444	0.443	0.002	282.6	0.482	0.484	0.004	281.5	0.555	0.555	0.000	281.8	0.447	0.443	0.009
280.1	0.370	0.369	0.011	281.1	0.345	0.350	0.014	281	0.503	0.499	0.004	280.9	0.364	0.363	0.003
279.3	0.297	0.307	0.034	279.8	0.248	0.251	0.012	280.1	0.408	0.411	0.007	279.5	0.248	0.250	0.008
278.1	0.241	0.244	0.012					279.3	0.350	0.347	0.009				
277.7	0.221	0.223	0.009					277.8	0.250	0.252	0.008				

$AD = \frac{|P_i^{cal} - P_i^{exp}|}{P_i^{exp}}$, *P*–represents the experimental and calculated pressure in MPa.

[a] U(T) (0.95 level of confidence) = 0.1 K, U(P) (0.95 level of confidence) = 0.007 MPa, U(w_i = mass fraction of salt) (0.95 level of confidence) = 0.0002 g. A precise analytical balance, model No. AV 114 (Ohaus Adventurer) with a manufacture error of ±0.0001 g in mass was utilized for the synthesis of the electrolyte mixtures. It should be noted that the salt concentrations in this study correspond to the (water + salt) system and the R507 is measured as a gas.
[b] Reference [11],
[c] Values are in mass fraction for water + salt.

Table 13
Experimental H–L_w–L_p –V (Hydrate – Aqueous Rich – Organic Rich – Vapour) Hydrate Dissociation Conditions for the R410a (1) + Water (2) + Salts (3) + CP (4) System at Industrial Salt Concentrations.[a]

R410a (1) + water (2) + 0.002[b] $CaCl_2$ (3) + 0.017[b] NaCl (4)				R410a (1) + water (2) + 0.002[b] $CaCl_2$ (3) + 0.017[b] NaCl (4) + CP (5)				R410a (1) + water (2) + 0.013[b] $MgCl_2$ (3) + 0.019[b] NaCl (4)				R410a (1) + water (2) + 0.013[b] $MgCl_2$ (3) + 0.019[b] NaCl (4) + CP (5)			
T/K	P^{exp}/MPa	P^{cal}/MPa	*AD*	*T*/K	P^{exp}/MPa	P^{cal}/MPa	*AD*	*T*/K	P^{exp}/MPa	P^{cal}/MPa	*AD*	*T*/K	P^{exp}/MPa	P^{cal}/MPa	*AD*
289.4	1.019	1.024	0.005	292.5	1.119	1.108	0.010	288.9	1.018	1.021	0.003	292.9	1.169	1.153	0.014
289.3	1.008	0.997	0.011	290.8	0.907	0.904	0.001	287.6	0.847	0.855	0.009	291.8	0.990	0.981	0.009
288.4	0.893	0.887	0.007	289.5	0.742	0.751	0.012	287.5	0.860	0.852	0.002	291.8	0.976	0.977	0.001
286.9	0.730	0.725	0.007	289.5	0.730	0.739	0.012	286.7	0.767	0.769	0.003	290.0	0.804	0.801	0.001
284.7	0.562	0.556	0.007	286.2	0.468	0.470	0.004	285	0.614	0.611	0.005	288.2	0.657	0.639	0.008
281.3	0.354	0.358	0.011	283.3	0.299	0.301	0.007	283.2	0.477	0.481	0.008	285.9	0.455	0.452	0.004
279.6	0.250	0.253	0.012					281.6	0.392	0.382	0.010	282.3	0.238	0.232	0.008
								279.1	0.244	0.245	0.004				

$AD = \frac{|P_i^{cal} - P_i^{exp}|}{P_i^{exp}}$, *P*–represents the experimental and calculated pressure in MPa.

[a] U(T) (0.95 level of confidence) = 0.1 K, U(P) (0.95 level of confidence) = 0.007 MPa, U(w_i = mass fraction of salt) (0.95 level of confidence) = 0.0002 g. A precise analytical balance, model No. AV 114 (Ohaus Adventurer) with a manufacture error of ± 0.0001 g in mass was utilized for the synthesis of the electrolyte mixtures. It should be noted that the salt concentrations in this study correspond to the (water + salt) system and the R410a is measured as a gas.
[b] Values are in mass fraction for water + salt.

Table 14
Experimental H–L_w–L_p –V (Hydrate – Aqueous Rich – Organic Rich – Vapour) Hydrate Dissociation Conditions for the R410a (1) + Water (2) + Salts (3) + CP (4) System at Higher Salt Concentrations.[a]

R410a (1) + water (2) + 0.080[b] $CaCl_2$ (3) + 0.050[b] NaCl (4)				R410a (1) + water (2) + 0.080[b] $CaCl_2$ (3) + 0.050[b] NaCl (4) + CP (5)				R410a (1) + water (2) + 0.150[b] $CaCl_2$ (3) + 0.050[b] NaCl (4)				R410a (1) + water (2) + 0.150[b] $CaCl_2$ (3) + 0.050[b] NaCl (4) + CP (5)			
T/K	P^{exp}/MPa	P^{cal}/MPa	*AD*	*T*/K	P^{exp}/MPa	P^{cal}/MPa	*AD*	*T*/K	P^{exp}/MPa	P^{cal}/MPa	*AD*	*T*/K	P^{exp}/MPa	P^{cal}/MPa	*AD*
288.8	1.067	1.059	0.007	291.7	1.099	1.089	0.009	282.2	1.074	1.064	0.009	289.4	1.041	1.023	0.017
288.8	1.083	1.067	0.006	289.8	0.809	0.799	0.012	281.8	0.996	0.986	0.010	286.6	0.742	0.734	0.011
286.6	0.809	0.811	0.002	288.4	0.664	0.662	0.003	280.6	0.811	0.805	0.007	286.8	0.761	0.756	0.007
284.6	0.651	0.646	0.008	286.4	0.499	0.505	0.012	280.7	0.832	0.823	0.011	285.1	0.621	0.615	0.010
282.9	0.532	0.533	0.002	286.4	0.513	0.508	0.010	279.7	0.699	0.696	0.004	282.8	0.466	0.457	0.004
281.2	0.437	0.440	0.007	283.2	0.314	0.316	0.006	279.3	0.648	0.647	0.002	280.2	0.306	0.301	0.013
279.3	0.351	0.355	0.011	280.6	0.191	0.193	0.010	277.9	0.519	0.525	0.012	278.1	0.204	0.199	0.020
276.4	0.246	0.243	0.016					276.1	0.374	0.378	0.011				
								274.5	0.279	0.283	0.014				

$AD = \frac{|P_i^{cal} - P_i^{exp}|}{P_i^{exp}}$, *P*–represents the experimental and calculated pressure in MPa.

[a] U(T) (0.95 level of confidence) = 0.1 K, U(P) (0.95 level of confidence) = 0.007 MPa, U(w_i = mass fraction of salt) (0.95 level of confidence) = 0.0002 g. A precise analytical balance, model No. AV 114 (Ohaus Adventurer) with a manufacture error of ± 0.0001 g in mass was utilized for the synthesis of the electrolyte mixtures. It should be noted that the salt concentrations in this study correspond to the (water + salt) system and the R410a is measured as a gas.
[b] Values are in mass fraction for water + salt.

CP, as a result R507 would not be suitable for gas hydrate technology for desalination process.

Fig. 11 presents system containing mixed electrolytes in the absence and presence of CP, then the (R410a + water + 0.002 mass fraction $CaCl_2$ + 0.017 mass fraction NaCl) system was measured at industrial maximum concentrations of electrolytes found in the wastewater and seawater [74-76]. It is revealed that in the presence of CP the hydrate dissociation temperatures increase by 2.4 K.

For the (R507 + water + 0.002 mass fraction $CaCl_2$ + 0.017 mass fraction NaCl + CP) system, it is found that the hydrate dissociation

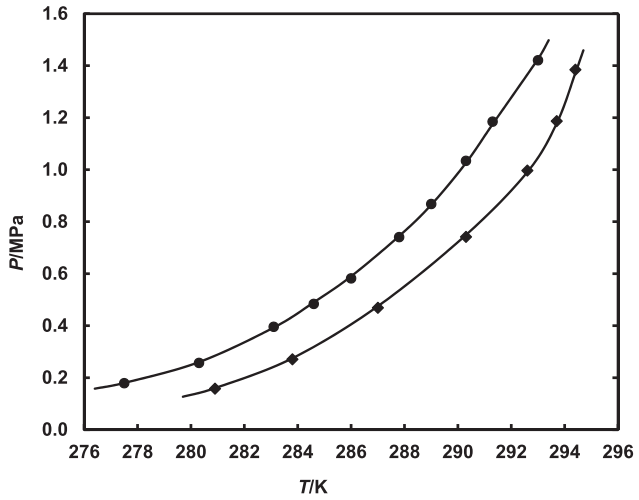

Fig. 6. Experimental and Estimated Hydrate Dissociation Conditions for the R410a (1) + Water (2) in the Absence and Presence of CP Systems: Symbols Represent Experimental Data: ●, Ngema *et al.* [11] in the Absence of CP; This Work: ◆, in the Presence of CP; ▬, Model Results.

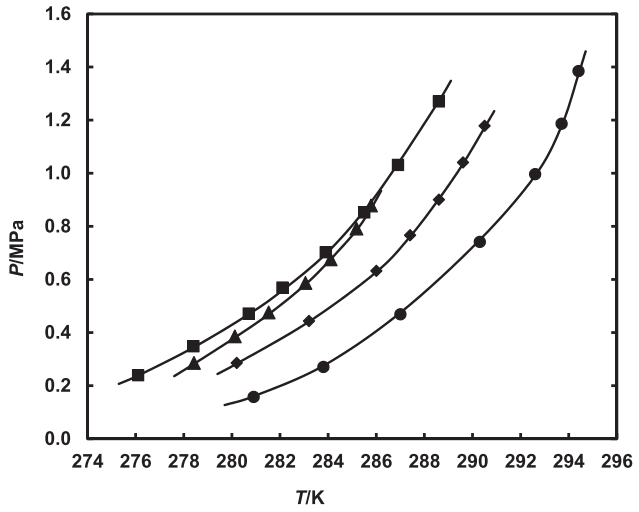

Fig. 7. Experimental and Estimated Hydrate Dissociation Conditions for the R410a (1) + Water (2) + NaCl (3) + CP (4) System: Symbols Represent Experimental Data: ■, Ngema *et al.* [11] [a]0.10 Mass Fraction in the Absence of Salt ; This Work: ●, in the Absence of Salt + CP; ◆, [a]0.10 Mass Fraction + CP; ▲, [a]0.20 Mass Fraction + CP; ▬, Model Results. [a]Values are in mass fraction for water + salt.

temperatures increase by 1.2 K at higher pressure of 0.759 MPa and increase by 1.7 K at lower pressure of 0.250 MPa as shown in Fig. 12. The (R410a + water + 0.013 mass fraction $MgCl_2$ + 0.019 mass fraction NaCl) shows an increase in the hydrate dissociation temperatures by 2.9 K at a higher pressure of 1.017 MPa and an increase by 3.2 K at lower pressure of 0.238 MPa as shown in Fig. 13.

At higher concentrations of 0.08 mass fraction of $CaCl_2$ and 0.05 mass fraction of NaCl, it is found that the hydrate dissociation temperatures increase by 3.2 K in the presence of CP as shown in Fig. 14. Further, increasing the concentration of $CaCl_2$ to 0.15 mass fraction and keeping NaCl at 0.05 mass fraction, it is also found that dissociation temperature increases by 7.6 K at higher pressure of 1.074 MPa and increases by 5.7 K at lower pressure of 0.279 MPa as shown in Fig. 15. All results for R410a systems show that it can be utilized as a potential hydrate former for gas hydrate technology for desalination processes due to their hydrate dissociation temperatures are close to ambient temperature.

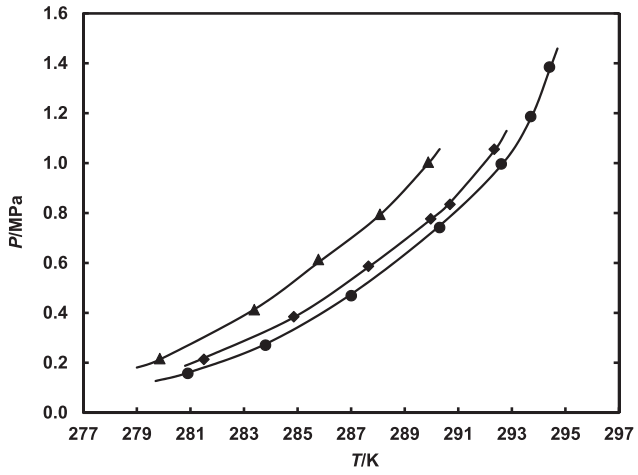

Fig. 8. Experimental and Estimated Hydrate Dissociation Conditions for the R410a (1) + Water (2) + $CaCl_2$ (3) + CP (4) System: Symbols Represent Experimental Data: This Work: ◆, in the Absence of Salt + CP; ●, [a]0.10 Mass Fraction + CP; ▲, [a]0.15 Mass Fraction + CP; ▬, Model Results. [a]Values are in mass fraction for water + salt.

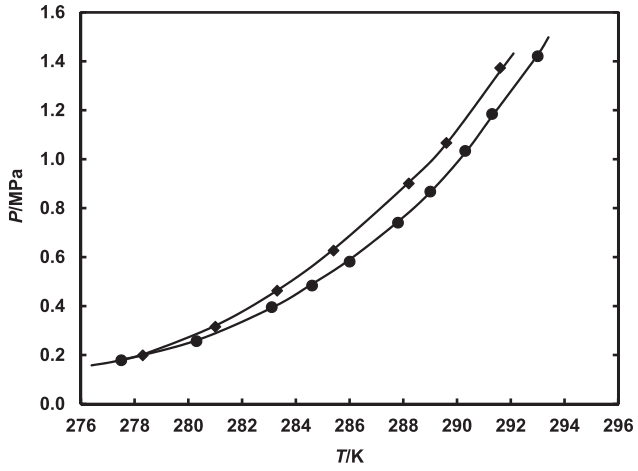

Fig. 9. Experimental and Estimated Hydrate Dissociation Conditions for the R410a (1) + Water (2) + Na_2SO_4 (3) System: Symbols Represent Experimental Data: ●, Akiya *et al.* [73] in the Absence of Salt; This Work: in the Presence of Salt: ◆, [a]0.10 Mass Fraction; ▬, Model Results. [a]Value is in mass fraction for water + salt.

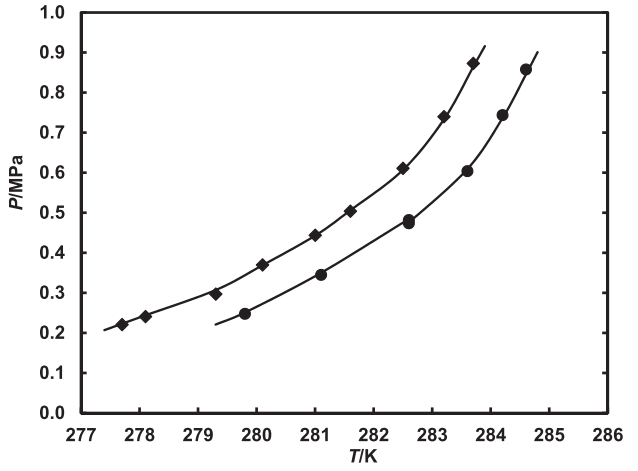

Fig. 10. Experimental and Estimated Hydrate Dissociation Conditions for the R507 (1) + Water (2) + CP (3) System: Symbols Represent Experimental Data: ◆, Ngema *et al.* [11] in the Absence of CP; This Work: ●, in the Presence of CP; ▬, Model Results.

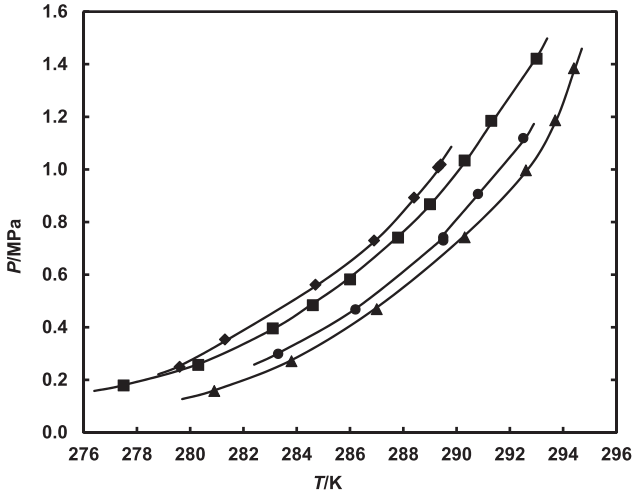

Fig. 11. Experimental and Estimated Hydrate Dissociation Conditions for the R410a (1) + Water (2) + [a]0.0020 Mass Fraction of $CaCl_2$ (3) + [a]0.017 Mass Fraction of NaCl (4) + CP (5) Systems: Symbols Represent Experimental Data: ■, Ngema *et al.* [11] in the Absence of Salt and CP; This Work: ◆, Mixed Salt in the Absence of CP; ●, Mixed Salt in the Presence of CP; ▲, R410a + Water + CP; ▬, Model Results. [a]Values are in mass fraction for water + salt.

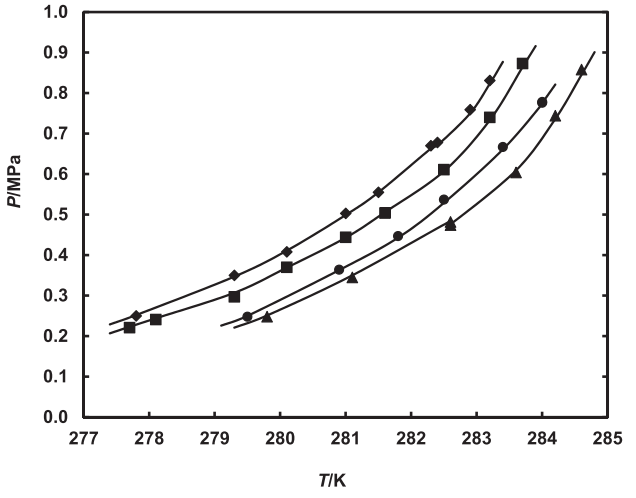

Fig. 12. Experimental and Estimated Hydrate Dissociation Conditions for the R507 (1) + Water (2) + [a]0.0020 Mass Fraction of $CaCl_2$ (3) + [a]0.017 Mass Fraction of NaCl (4) + CP (5) System: Symbols Represent Experimental Data: ■, Ngema *et al.* [11] in the Absence of CP; This Work: ◆, Mixed Salt in the Absence of CP; ●, Mixed Salt in the Presence of CP; ▲, R507 + Water + CP; ▬, Model Results. [a]Values are in mass fraction for water + salt.

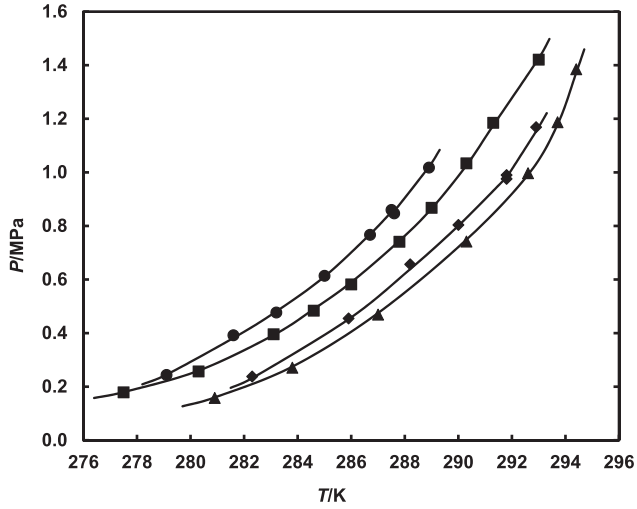

Fig. 13. Experimental and Estimated Hydrate Dissociation Conditions for the R410a (1) + Water (2) + [a]0.013 Mass Fraction of $MgCl_2$ (3) + [a]0.019 Mass Fraction of NaCl (4) + CP (5) System: Symbols Represent Experimental Data: ■, Ngema *et al.* [11] in the Absence of CP; This Work:●, Mixed Salt in the Absence of CP; ◆, Mixed Salt in the Presence CP; ▲, R410a in the Presence of CP; ▬, Model Results. [a]Values are in mass fraction for water + salt.

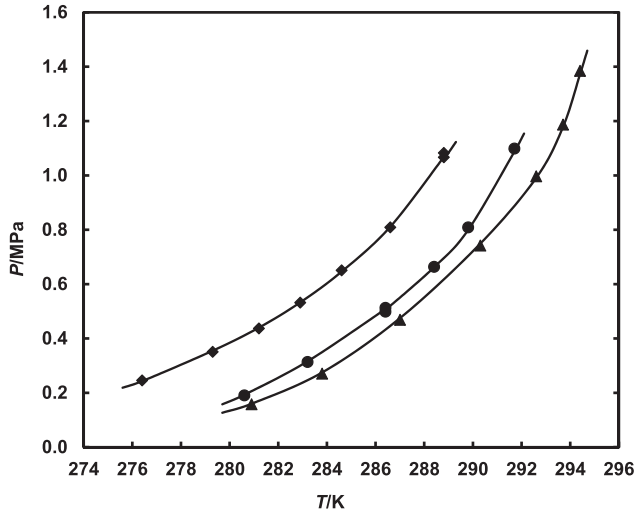

Fig. 14. Experimental and Estimated Hydrate Dissociation Conditions for the R410a (1) + Water (2) + [a]0.08 Mass Fraction of $CaCl_2$ (3) + [a]0.05 Mass Fraction of NaCl (4) + CP (5) System: Symbols Represent Experimental Data: This Work: ▲, R410a in the Presence of CP; ◆, Mixed Salt in the Absence of CP; ●, Mixed Salt in the Presence of CP; ▬, Model Results. [a]Values are in mass fraction for water + salt.

4.2. HE–CPA equation of state model

The measured systems were modelled using a combination of various contributions in order to completely develop a HE–CPA equation of state as presented in Eq. (1). The modelling of the electrolyte systems is based on the assumptions that no ions are present in the vapour phase and electrolyte does not enter the hydrate phase.

The HE–CPA equation of state was first tested using known systems for {(R410a or R134a or R507) + water} from literature [73,77]. Figs. 5, 6 and 10 show that the model results strongly agree with literature [73,77] hydrate dissociation data. Furthermore, it is noted that the HE–CPA model shows impressive results for measured hydrate systems for {R410a + water + single and mixed electrolytes (NaCl, $CaCl_2$, $MgCl_2$ and Na_2SO_4)} in the absence and presence of CP, as shown in Figs. 6–15. The results obtained show that R410a is a suitable fluorinated refrigerant to be employed in a water desalination process. R410a shows impressive hydrate dissociation temperatures near ambient temperatures.

Tables 15 presents the Langmuir constant parameters (*c and d*) for the (refrigerant + water) system were achieved by using Eq. (27), then, the obtained Langmuir constant parameters were regressed using the measured hydrate dissociation data in the presence of pure water. Eq. (27) was selected to be used to determine parameters R410a and R507 because these fluorinated refrigerants have large molecules, thus, they cannot inter the small cavities of their applicable gas hydrate structures. The constant parameters were determined based on the assumption that R410a and R507 are pure gases.

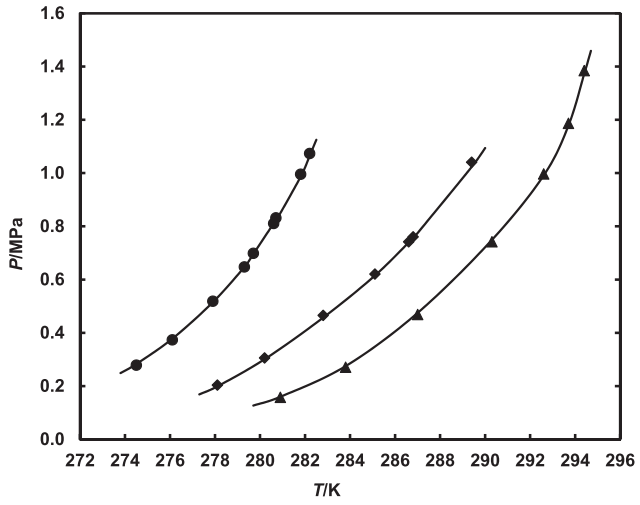

Fig. 15. Experimental and Estimated Hydrate Dissociation Conditions for the R410a (1) + Water (2) + [a]0.15 Mass Fraction of $CaCl_2$ (3) + [a]0.05 Mass Fraction of NaCl (4) + CP (5) System: Symbols Represent Experimental Data: This Work: ▲, R410a in the Presence of CP; ●, Mixed Salt in the Absence of CP; ◆, Mixed Salt in the Presence of CP; ▬, Model Results. [a]Values are in mass fraction for water + salt.

Table 15
Langmuir Constants Parameters Used in this Study.

Hydrate systems	C′/(K·MPa^{-1})	d′/K
[a]R134a	5.700×10^{-3}	4908.75
[a]R410a	4.750×10^{-3}	5969.68
[a]R507	4.500×10^{-4}	6233.08
Cyclopentane	2.156 x10^{-4}	5950

c′ and *d*′ are the adjustable parameters for the Langmuir constant.
[a] Rerefence[11].

Table 16
Average Absolute Deviation (AAD) for R410a and R507 Measured Systems in the Presence of Salt and Promoter.

Measured Systems	AAD
[a]R410a (1) + water (2)	0.008
R410a (1) + water (2) + CP (3)	0.010
R410a (1) + water (2) + 0.100 NaCl (3)	0.008
R410a (1) + water (2) + 0.100 NaCl (3) + CP (4)	0.009
R410a (1) + water (2) + 0.200 NaCl (3) + CP (4)	0.010
R410a (1) + water (2) + 0.100 $CaCl_2$ (3) + CP (4)	0.009
R410a (1) + water (2) + 0.150 $CaCl_2$ (3) + CP (4)	0.010
R410a (1) + water (2) + 0.100 Na_2SO_4 (3)	0.008
[b]R134a (1) + water (2)	0.008
[a]R507 (1) + water (2)	0.010
R507 (1) + water (2) + CP (3)	0.009
R507 (1) + water (2) + 0.002 $CaCl_2$ (3) + 0.017 NaCl (4)	0.008
R507 (1) + water (2) + 0.002 $CaCl_2$ (3) + 0.017 NaCl (4) + CP (5)	0.007
R410a (1) + water (2) + 0.002 $CaCl_2$ (3) + 0.017 NaCl (4)	0.009
R410a (1) + water (2) + 0.002 $CaCl_2$ (3) + 0.017 NaCl (4) + CP (5)	0.008
R410a (1) + water (2) + 0.013 $MgCl_2$ (3) + 0.019 NaCl (4)	0.006
R410a (1) + water (2) + 0.013 $MgCl_2$ (3) + 0.019 NaCl (4) + CP (5)	0.006
R410a (1) + water (2) + 0.080 $CaCl_2$ (3) + 0.050 NaCl (4)	0.007
R410a (1) + water (2) + 0.080 $CaCl_2$ (3) + 0.050 NaCl (4) + CP (5)	0.009
R410a (1) + water (2) + 0.150 $CaCl_2$ (3) + 0.050 NaCl (4)	0.008
R410a (1) + water (2) + 0.150 $CaCl_2$ (3) + 0.050 NaCl (4) + CP (5)	0.009

$AAD\% = \frac{100}{N}\sum_i^N \frac{|p_i^{cal} - p_i^{exp}|}{p_i^{exp}}$, *P*–present the experimental and estimated pressure in MPa.
[a] Reference [11],
[b] Reference [96].

In the HE–CPA model used, it is revealed that the model provides an adequate illustration of the measured hydrate dissociation data. The average absolute deviation (AAD), in Eq. (28) was used to minimize the *c* and *d* parameters for the HE–CPA model. Table 16 presents the calculated average absolute deviations for all measured hydrate dissociation data, which shows a good agreement between the measured and estimated hydrate dissociation conditions. The measured pressures are within uncertainty as they show errors less than 1%, which indicate that the results are satisfactory. Consequently, the HE–CPA model can be used to predict any systems of interest as it leads to satisfactory predictions as shown in Figs. 5–15.

$$AAD(\%) = \frac{100}{N}\sum_i^N \left|\frac{P_i^{exp} - P_i^{cal}}{P_i^{exp}}\right| \tag{33}$$

where *N* represents the quantity of hydrate dissociation data points, subscript *i* referred to *i*th experimental and calculated hydrate dissociation data points and superscript "exp" and "*cal*" are experimental and calculated hydrate dissociation data points, respectively.

4.3. Enthalpy of hydrate dissociation

The energy required for the hydrate systems containing electrolytes is determined by the enthalpy of hydrate dissociation. It is an essential property for the design of a gas hydrate based desalination process. The Clausius-Clapeyron equation was used to estimate enthalpy of hydrate dissociation.

$$\Delta H = -RZ\left(\frac{d(\ln P)}{d\left(\frac{1}{T}\right)}\right) \tag{34}$$

where Z represents the compressibility factor, which is calculated by using SRK equation of state [54], *R* represents universal gas constant and d(lnP)/d(1/T) is the gradient obtained by plotting lnP vs 1/T using experimental hydrate dissociation data. Table 17 presents the calculated values for enthalpy of dissociation that have been plotted in Fig. 16. Three hydrate formers are reported in Table 17 (R410a, R507 and R134a). From Fig. 16, it is observed that R507 systems have high enthalpy compare to R134 and R410a. It is noted that the measured dissociation temperatures for R507 systems are lower than R410a systems. This shows that more energy is required for R507, consequently, it is not a suitable hydrate former for a hydrate based desalination process as well as R134a for the same reasons.

5. Conclusion

Hydrate dissociation conditions measurements indicate that R410a in the presence of CP has a potential to be used for gas hydrate based water desalination processes. Cyclopentane shows impressive results to shift the hydrate phase boundary to near ambient temperature. The results show that R507 is not suitable for gas hydrate based water desalination processes since the hydrate dissociation temperatures are not close to ambient temperature even in the presence of CP. The measured hydrate dissociation data in the absence and presence of single and mixed salts were satisfactorily correlated with a developed HE–CPA equation of state based model. In the HE–CPA model, the hydrate phase is modeled using the solid solution theory of van der Waals and Platteeuw [50], the electrolyte aqueous system is modeled using Deybe–Hückel [49], and the CPA [51] equation of state is used for modeling liquid or vapour phase. This model is reliable and provides acceptable results as it shows the average absolute deviations that are less than 1%.

The enthalpy of hydrate dissociation was calculated using Clausius-Clapeyron equation. It was revealed that hydrate formers (R507 and R134a) are not suitable for hydrate based water

Table 17
Estimated Enthalpy of Hydrate Dissociation.

R410a (1) + water (2)

T(K)	ΔH/(kJ·mol^{-1})
293.0	69.58
291.3	75.91
290.3	78.04
289.0	80.31
287.8	81.99
286.0	84.07
284.6	85.33
283.1	86.46
280.3	88.26
277.5	89.26

R134a (1) + water (2)

T/K	ΔH/(kJ·mol^{-1})
283.0	124.15
282.6	125.38
281.9	126.85
281.4	128.24
281.4	128.37
280.7	129.29
280.4	129.73
280.0	130.34
280.0	130.45
279.3	131.37
278.4	132.59
277.6	133.25
275.8	134.25

R410a (1) + water (2) + 0.1NaCl (3)

T/K	ΔH/(kJ·mol^{-1})
288.6	69.94
286.9	73.31
285.5	75.73
283.9	77.67
282.1	79.36
280.7	80.61
278.4	82.17
276.1	83.56

R410a (1) + water (2) + 0.1NaCl (3) + CP (4)

T/K	ΔH/(kJ·mol^{-1})
290.5	76.21
289.6	78.19
288.6	80.16
287.4	81.97
286.0	83.75
283.2	86.21
280.2	88.28

R410a (1) + water (2) + 0.2NaCl (3) + CP (4)

T/K	ΔH/(kJ·mol^{-1})
285.8	85.11
285.2	86.44
283.1	89.43
281.5	91.01
280.1	92.29
278.4	93.73

R410a (1) + water (2) + 0.1$CaCl_2$ (3) + CP (4)

T/K	ΔH/(kJ·mol^{-1})
293.7	109.33
292.7	113.48
292.0	114.48
290.2	117.83
290.2	117.62
287.9	121.35
285.3	124.33

R410a (1) + water (2) + 0.15$CaCl_2$ (3) + CP (4)

T/K	ΔH/(kJ·mol^{-1})
291.9	95.94
290.1	99.28
287.7	102.35
287.8	102.08
285.4	105.22
282.6	108.35

R410a (1) + water (2) + 0.1Na_2SO_4 (3)

T/K	ΔH/(kJ·mol^{-1})
291.6	77.33
289.6	82.07
288.2	84.50
285.4	88.39
283.3	90.68
283.3	90.97
281.0	92.72
278.3	94.35

R410a (1) + water (2) + 0.05NaCl (3) + 0.08$CaCl_2$ (4)

T/K	ΔH/(kJ·mol^{-1})
288.8	66.21
288.8	66.00
286.6	69.28
284.6	71.08
282.9	72.42
281.2	73.48
279.3	74.44
276.4	75.63

R410a (1) + water (2) + 0.05NaCl (3) + 0.08$CaCl_2$ (4) + CP (5)

T/K	ΔH/(kJ·mol^{-1})
294.6	93.04
292.7	97.60
291.2	99.76
289.2	101.99
289.2	102.20
286.2	104.93
283.8	106.77

R410a (1) + water (2) + 0.05NaCl (3) + 0.15$CaCl_2$ (4)

T/K	ΔH/(kJ·mol^{-1})
282.2	90.75
281.8	92.24
280.6	95.65
280.7	95.26
279.7	97.63
279.3	98.53
277.3	100.69
276.1	103.21
274.5	104.81

R410a (1) + water (2) + 0.05NaCl (3) + 0.15$CaCl_2$ (4) + CP (5)

T/K	ΔH/(kJ·mol^{-1})
289.4	92.47
286.6	97.29
286.6	96.96
285.1	99.19
283.4	101.64
281.1	104.15
279.3	105.75

R410a (1) + water (2) + 0.002$CaCl_2$ (3) + 0.017NaCl (4)

T/K	ΔH/(kJ·mol^{-1})
289.3	103.11
289.4	102.92
288.4	105.11
284.7	110.71
281.3	114.20
279.6	115.96

R410a (1) + water (2) + 0.002$CaCl_2$ (3) + 0.017NaCl (4) + CP (5)

T/K	ΔH/(kJ·mol^{-1})
292.5	105.17
290.8	108.89
289.5	111.77
289.5	111.99
286.2	116.40
283.3	119.25

R410a (1) + water (2) + 0.0013$MgCl_2$ (3) + 0.019NaCl (4

T/K	ΔH/(kJ·mol^{-1})
288.9	105.81
287.6	108.90
287.5	108.64
286.7	110.30
285	112.97
283.2	115.34
281.6	116.80
279.1	119.40

R410a (1) + water (2) + 0.0013$MgCl_2$ (3) + 0.019NaCl (4) + CP (5)

T/K	ΔH/(kJ·mol^{-1})
292.9	108.66
291.8	112.03
291.8	112.29
290.0	115.35
288.2	117.93
285.9	121.51
282.3	125.36

R507 (1) + water (2)

T/K	ΔH/(kJ·mol^{-1})
283.3	126.46
283.0	131.25
282.2	135.55
281.3	138.96
280.7	140.84
280.0	143.14
279.0	145.35
278.1	147.04
277.7	147.64

R507 (1) + water (2) + CP (3)

T/K	ΔH/(kJ·mol^{-1})
284.6	139.76
284.2	144.12
283.2	149.11
282.6	153.68
282.6	153.39
281.1	157.95
279.8	161.13

R507 (1) + water (2) + 0.002$CaCl_2$ (3) + 0.017NaCl (4)

T/K	ΔH/(kJ·mol^{-1})
283.0	162.45
282.9	165.53
282.4	168.79
282.3	169.09
281.5	173.60
281.0	175.62
280.1	179.17
279.3	181.32
277.8	185.02

R507 (1) + water (2) + 0.002$CaCl_2$ (3) + 0.017NaCl (4) + CP (5)

T/K	ΔH/(kJ·mol^{-1})
284.0	186.96
284.1	187.23
283.4	191.99
282.5	197.66
281.8	201.50
280.9	204.96
279.5	209.77

Table 17 (*continued*)

R410a (1) + water (2) + CP (3)	
T(K)	ΔH (kJ.mol^{-1})
294.4	85.70
293.7	89.10
292.6	92.14
290.3	96.01
287.0	100.03
283.8	102.95
280.9	104.62

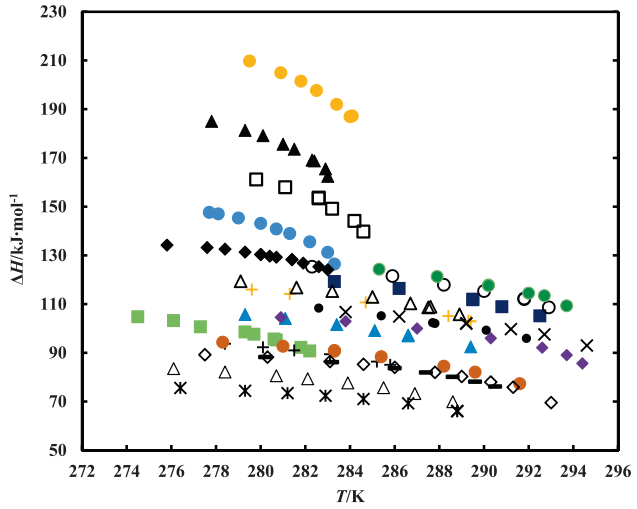

Fig. 16. Estimated Enthalpy of Hydrate Dissociation: This work: ◇, A; ◆, B; Δ, C; ▬, D; +, E; ●, F; ●, G; ●, H; *, I; ×, J; ■, K; ▲, L; +, M; ■, N; Δ, O; ○, P; ●, Q; □, R; ▲, S; ●, T; ◆, U. A: R410a (1) + water (2); B: R134a (1) + water (2); C: R410a (1) + water (2) + [a]0.1NaCl (3); D: R410a (1) + water (2) + [a]0.1NaCl (3) + CP (4); E: R410a (1) + water (2) + [a]0.2NaCl (3) + CP (4); F: R410a (1) + water (2) + [a]0.1$CaCl_2$ (3) + CP (4); G: R410a (1) + water (2) + [a]0.15$CaCl_2$ (3) + CP (4); H: R410a (1) + water (2) + [a]-0.1Na_2SO_4 (3); I: R410a (1) + water (2) + [a]0.05NaCl (3) + [a]0.08$CaCl_2$ (4); J: R410a (1) + water (2) + [a]0.05NaCl (3) + [a]0.08$CaCl_2$ (4) + CP (5); K: R410a (1) + water (2) + [a]-0.05NaCl (3) + [a]0.15$CaCl_2$ (4); L: R410a (1) + water (2) + [a]0.05NaCl (3) + [a]0.15$CaCl_2$ (4) + CP (5); **M:** R410a (1) + water (2) + [a]0.002$CaCl_2$ (3) + [a]0.017NaCl (4); N: R410a (1) + water (2) + [a]0.002$CaCl_2$ (3) + [a]0.017NaCl (4) + CP (5); O: R410a (1) + water (2) + [a]0.0013$MgCl_2$ (3) + [a]0.019NaCl (4); P: R410a (1) + water (2) + [a]0.0013$MgCl_2$ (3) + [a]0.019NaCl (4) + CP (5); Q: R507 (1) + water (2); R: R507 (1) + water (2) + CP (3); S: R507 (1) + water (2) + [a]0.002$CaCl_2$ (3) + [a]0.017NaCl (4); T: R507 (1) + water (2) + [a]0.002$CaCl_2$ (3) + [a]0.017NaCl (4) + CP (5); **U:** R410a (1) + water (2) + CP (3). [a]-Values are in mass fraction for water + salt.

desalination processes as they have higher enthalpies compared to R410a. This shows that more energy is required for R507 and R134a hydrates.

Acknowledgement

This study was supported by the South African Research Chairs Initiative of the Department of Science and Technology and National Research Foundation. The authors would like to thank the NRF Focus Area Programme and the NRF Thuthuka Programme.

Appendix A. Supplementary data

Supplementary data to this article can be found online at https://doi.org/10.1016/j.jct.2019.04.012.

References

[1] A.H. Mohammadi, D. Richon, Ind. Eng. Chem. Res. 49 (2010) 925–928.
[2] K. Tumba, P. Reddy, P. Naidoo, D. Ramjugernath, A. Eslamimanesh, A.H. Mohammadi, D. Richon, J. Chem. Eng. Data 56 (2011) 3620–3629.
[3] E.D. Sloan, C.A. Koh, Clathrate Hydrates of Natural Gases, 3rd ed., CRC Press, Taylor & Francis Group, London, New York, 2008.
[4] J. Javanmardi, M. Moshefeghian, Appl. Thermodyn. Eng. 23 (2003) 845–857.
[5] C.P. Huang, O. Fennema, W.D. Poweri, Cryobiology 2 (1966) 240–245.
[6] A. Eslamimanesh, A.H. Mohammadi, D. Richon, P. Naidoo, D. Ramjugernath, J. Chem. Thermodyn. 46 (2012) 62–71.
[7] K. Park, S.Y. Hong, J.W. Lee, K.C. Kang, Y.C. Lee, M.-G. Ha, J.D. Lee, Desalination 274 (2011) 91–96.
[8] J.A. Ripmeester, J.S. Tse, C.I. Rateliffe, Nature 328 (1987) 469–478.
[9] A.D. Khawaji, I.K. Kutubkhanaha, J.-M. Wie, Desalination 221 (2008) 47–69.
[10] S.A. Kalogirou, Prog. Energy Combust. Sci. 31 (2005) 242–281.
[11] P.T. Ngema, C. Petticrew, P. Naidoo, A.H. Mohammadi, D. Ramjugernath, J. Chem. Eng. Data 59 (2014) 466–475.
[12] P.T. Ngema, P. Naidoo, A.H. Mohammadi, D. Richon, D. Ramjugernath, J. Chem. Eng. Data 61 (2016) 466–475.
[13] P.T. Ngema, P. Naidoo, A.H. Mohammadi, D. Richon, D. Ramjugernath, Fluid Phase Equilib. 413 (2016) 92–98.
[14] J. Sugi, S. Saito, Desalination 3 (1967) 27–31.
[15] R.A. McCormack, R.K. Anderso, Clathrate desalination plants preliminary research study, Water Treatment Technology Program Report No. 5, Thermal Energy Storage, Inc., San Diege, CA, 1995.
[16] A.J. McCormack, G.A. Niblock, Build and operate a clathrate desalination pilot plant, Water Treatment Technology Program Report No. 31, Thermal Energy Storage, Inc., San Diege, CA, 1998.
[17] A.J. Barduhn, Chem. Eng. Prog. 63 (1967) 98–103.
[18] H. Kubota, K. Shimizu, Y. Tanaka, T. Makita, J. Chem. Eng. Jpn. 17 (1984) 423–429.
[19] J.H. Cha, Y. Seol, Sustainable Chem. Eng. 1 (2013) 1218–1224.
[20] D. Corak, T. Barth, S. Hoiland, T. Skodvin, R. Larsen, T. Skjetne, Desalination 278 (2011) 268–274.
[21] R.W. Bradshaw, J.A. Greathouse, R.T. Cygan, B.A. Simmons, D.E. Dedrick, E.H. Majzoub, Desalination utilizing gas hydrates, LDRD Final Report, Sandia National laboratories, Albuquerque, NM, 2008.
[22] P.T. Ngema, MSc Thesis in Chemical Engineering, University of KwaZulu-Natal, Durban, South Africa, 2014.
[23] K.-H. Guo, B.-F. Shu, Z.-X. Meng, L. Zeng, Chinese Patent No. ZL95107268.4, 1995.
[24] K.-H. Guo, B.-F. Shu, W.-J. Yang, Proceedings of 1st Trabzon Int. Energy and Environment Symposium vol. 1 (1996) 381–386.
[25] A. Eslamimanesh, A.H. Mohammadi, D. Richon, Chem. Eng. Sci. 66 (2011) 5439–5445.
[26] M.-K. Chun, H. Lee, B.J. Ryu, J. Chem. Eng. Data 45 (2000) 1150–1153.
[27] Y. Seo, H. Lee, Environ. Sci. Technol. 35 (2001) 3386–3390.
[28] P. Ilani-Kashkouli, S. Babaee, F. Gharagheizi, H. Hashemi, A.H. Mohammadi, D. Ramjugernath, Fluid Phase Equilib. 360 (2013) 68–76.
[29] Y. Kamata, H. Oyama, W. Shimada, T. Ebinuma, S. Takeya, T. Uchida, J. Nagao, H. Narita, J. Jap, App. Phys 43 (2004) 362–365.
[30] H.Y. Acosta, P.B. Bishnoi, M.A. Clarke, J. Chem. Eng. Data 56 (1) (2011) 69–73.
[31] J. Deschamps, D. Dalmazzone, J. Chem. Eng. Data 55 (9) (2010) 3395–3399.
[32] S. Li, S. Fan, J. Wang, X. Lang, Y. Wang, J. Chem. Eng. Data 55 (9) (2010) 3212–3215.
[33] M. Oshima, W. Shimada, S. Hashimoto, A. Tani, K. Ohgaki, Chem. Eng. Sci. 65 (2010) 5442–5446.
[34] T. Rodionova, V. Komarov, G. Villevald, I. Aladko, T. Karpova, A. Manakov, J. Phys. Chem. B 114 (2010) 11838–11846.
[35] T. Sugahara, J.C. Haag, A.A. Warntjes, P.S.R. Prasad, E.D. Sloan, C.A. Koh, A.K. Sum, J. Phys. Chem. C 114 (2010) 15218–15222.
[36] Z.G. Sun, L. Sun, J. Chem. Eng. Data 55 (2010) 3538–3541.
[37] A.K. Sum, C.A. Koh, E.D. Sloan, Ind. Eng. Chem. Res. 48 (2009) 7457–7465.
[38] B. Castellania, M. Fillipponib, S. Rinaldia, F. Rossib, Capture of carbon dioxide using gas hydrate technology, The 25th International Conference on efficiency, Cost, Optimization and Environmental Impact of Energy Systems, Perugia, Italy, 2012.
[39] D.D. Link, E.P. Ladner, H.A. Elsen, C.E. Taylor, Fluid Phase Equilib. 211 (2003) 1–10.
[40] W. Lin, G.J. Chen, C.Y. Sun, X.Q. Guo, Z.K. Wu, M.Y. Liang, Chem. Eng. Sci. 59 (2004) 4449–4455.
[41] J. Yoslim, P. Linga, P. Engelos, J. Cryst. Growth 313 (2010) 68–80.

[42] H. Roosta, S. Khosharay, F. Varaminian, Energy Conv. Manage. 76 (2013) 499–505.
[43] Z. Sun, R. Wang, R. Ma, K. Guo, S. Fan, Energy Convers. Manage. 44 (2003) 2733–2740.
[44] W. Hao, J. Wang, S. Fan, W. Hao, Energy Convers. Manage. 49 (2008) 2546–2553.
[45] A.H. Mohammadi, D. Richon, AIChE Annual Meeting, Proceeding, Salt Lake City, UT, 2010.
[46] A.H. Mohammadi, D. Richon, J. Thermodyn (2009) 1–12.
[47] P.J. Herslund, Phd Thesis, Center for Energy Resources Engineering, Department of Chemical and Biochemical Engineering, Technical University of Denmark, Denmark, 2013.
[48] Z.-Y. Chen, Q.-P. Li, Z.-Y. Yan, K.-F. Yan, Z.-Y. Zeng, X.-S. Li, J. Chem. Eng. Data 55 (2010) 4444–4449.
[49] P. Deybe, E. Hückel, Z. Phys. 24 (1923) 179–207.
[50] J.H. van der Waals, J.C. Platteeuw, Adv. Chem. Phys. 2 (1959) 1–57.
[51] G.M. Kontogeorgis, E.C. Voutas, I.V. Yakoumis, D.P. Tassios, Ind. Eng. Chem. Res. 35 (1996) 4310–4318.
[52] A.H. Mohammadi, W. Afzal, D. Richon, J. Chem. Thermodyn. 40 (2008) 1693–1697.
[53] B. Maribo-Mogensen, PhD Thesis, Center for Energy Resources Engineering, Department of Chemical and Biochemical Engineering, Technical University of Denmark, Denmark, 2014.
[54] G. Soave, Chem. Eng. Sci. 27 (6) (1972) 1197–1203.
[55] G.M. Kontogeorgis, G.K. Folas, Thermodynamic Models for Industrial Applications: From Classical and Advanced Mixing Rules to Association Theories, Wiley, Ltd, Publication, 2010.
[56] G.M. Kontogeorgis, M.L. Michelsen, G.K. Folas, S. Derewi, N. von Solms, E.H. Stenby, Ind. Eng. Chem. Res. 45 (2006) 4855–4868.
[57] G.M. Kontogeorgis, M.L. Michelsen, G.K. Folas, S. Derewi, N. von Solms, E.H. Stenby, Ind. Eng. Chem. Res. 45 (2006) 4869–4878.
[58] G.M. Kontogeorgis, I.V. Yakoumis, H. Meijer, E. Hendriks, T. Moorwood, Fluid Phase Equilib. 158–160 (1999) 201–209.
[59] H. Haghighi, A. Chapoy, B. Tohidi, Oil Gas Sci. Technol. 64 (2) (2009) 141–154.
[60] S.H. Huang, M. Radosz, Ind. Eng. Chem. Res. 29 (1990) 2284–2294.
[61] E.C. Voutsas, I.V. Yakoumis, D.P. Tassios, Fluid Phase Equilib. 158–160 (1999) 151–160.
[62] E.C. Voutsas, G.C. Boulougouris, I.G. Economou, D.P. Tassios, Ind. Eng. Chem. Res. 39 (2000) 797–809.
[63] S.O. Derawi, G.M. Kontogeorgis, M.L. Michelsen, E.H. Stenby, Ind. Eng. Chem. Res. 42 (2003) 1470–1479.
[64] G. K. Folas, PhD Thesis, Center for Energy Resources Engineering, Department of Chemical Engineering, Technical University of Denmark, Denmark, 2006.
[65] M.L. Michelsen, J.M. Mollerup, Thermodynamics Models: Fundamentals and Computational Aspects, second ed., Tie-Line Publication, 2007.
[66] Y. Lin, A. Kate, M. Mooijer, J. Delgado, P.L. Fosbol, K. Thomsen, AIChE J. 56 (5) (2010) 1334–1351.
[67] J. Gmehling, B. Kolbe, M. Kleiber, J. Rarey, Chemical Thermodynamics for Process Simulation, Wiley-VCH Verlag GmbH & Co, KGaA, 2012.
[68] K. Thomsen, Electrolyte solutions: Thermodynamics, crystallization, separation methods, Technical University of Denmark, Department of Chemical Engineering, 2009.
[69] G.N. Lewis, M. Randall, J. Am. Chem. Soc. 43 (1921) 1112–1154.
[70] W.R. Parrish, J.M. Prausnitz, Ind. Eng. Chem. 11 (1) (1972) 26–35.
[71] R. Döring, H. Buchwald, J. Hellmann, Int. J. Refrig. 20 (2) (1997) 78–84.
[72] J.E. Calm, Refrig. Manage. Serv (2008) 1–14.
[73] T. Akiya, T. Shimazaki, M. Oowa, M. Matsuo, Y. Yoshida, Int. J. Thermophys. 20 (1999) 1753–1763.
[74] D. Lalla, D. Raman, J. Hofmann, in: Tutuka Power Station Brine Concentration Plant, Eskom holdings SOC LTD, 2014, pp. 1–9.
[75] B. Dalmacija, E. Karalovic, Z. Tamas, D. Miskovic, Wat. Res 30 (1996) 295–298.
[76] A. Lewis, J. Nathoo, T. Reddy, D. Randall, L. Zibi, R. Jivanji, Wat. Res. Comm (2010) 1–82.
[77] D. Liang, K. Guo, R. Wang, S. Fan, Fluid Phase Equilib. 187–188 (2001) 61–70.
[78] P. Englezos, Y.T. Ngan, J. Chem. Eng. Data 38 (1993) 250–253.
[79] B. Tohidi, R.W. Burgrass, A. Danesh, K.K. Østergaard, A.C. Todd, Ann. N. Y. Acad. Sci. 912 (2000) 924–931.
[80] J. Javanmardi, M. Moshefeghian, R.N. Maddox, Energy Fuels 12 (1998) 219–222.
[81] B.E. Poling, J.M. Prausnitz, J.P. O'Connell, The Properties of Gases and Liquids, fifth ed., McGraw-Hill, New York, 2001.
[82] A.A. Macedo, P. Skovborg, P. Rasmussen, Chem. Eng. Sci. 45 (4) (1990) 875–882.
[83] Y.I. Shouzhi, J.I.A. Yuanyuan, M.A. Peisheng, Chin.J Chem. Eng. 13 (5) (2005) 709–712.
[84] C.C. Chen, L.B. Evans, AIChE J. 32 (3) (1986) 444–454.
[85] Y. Song, C.C. Chen, Ind. Eng. Chem. Res 48 (16) (2009) 7788–7797.
[86] K.S. Pitzer, J.M. Simonson, J. Phys. Chem 90 (13) (1986) 3005–3009.
[87] M. Born, Z. Phys 1 (1920) 45–68.
[88] P. Wang, A. Anderko, R.D. Young, Fluid Phase Equilib. 203 (1) (2002) 141–176.
[89] P. Wang, R.D. Springer, A. Anderko, R.D. Young, Fluid Phase Equilib. 222 (2004) 11–17.
[90] P. Wang, A. Anderko, R.D. Springer, R.D. Young, J. Mol. Liq. 125 (1) (2006) 37–44.
[91] P. Wang, J.J. Kosinski, M.M. Lencka, A. Anderko, R.D. Springer, Pure App. Chem 85 (11) (2013) 2117–2144.
[92] A. Anderko, P. Wang, M. Rafal, Fluid Phase Equilib. 194 (2002) 132–142.
[93] D.S. Abrams, J.M. Prausnitz, AIChE J. 21 (1) (1975) 116–128.
[94] K.S. Pitzer, J. Phys. Chem. 77 (2) (1973) 268–277.
[95] K. Thomsen, P. Rasmussen, R. Gani, Chem. Eng. Sci. 51 (14) (1996) 3675–3683.
[96] K. Thomsen, P. Rasmussen, Chem. Eng. Sci. 54 (12) (1999) 1787–1802.

JCT 2018-801